

1 **New data on flatfish scuticociliatosis reveal**
2 **that *Miamiensis avidus* and *Philasterides***
3 ***dicentrarchi* are different species**

4 ANA-PAULA DEFELIPE¹, JESÚS LAMAS², ROSA-ANA SUEIRO^{1,2},
5 IRIA FOLGUEIRA¹ and JOSÉ-MANUEL LEIRO^{1*}

6 ¹*Departamento de Microbiología y Parasitología, Instituto de Investigación y Análisis Alimentarios,*
7 *Universidad de Santiago de Compostela, 15782 Santiago de Compostela, Spain*

8 ²*Departamento de Biología Celular y Ecología, Instituto de Acuicultura, Universidad de Santiago de*
9 *Compostela, 15782 Santiago de Compostela, Spain*

10

11

12

13

14

15 SHORT TITLE: Scuticociliatosis in flatfish

16

17

18

19

20

21 * **Correspondence**

22 José M. Leiro, Laboratorio de Parasitología, Instituto de Investigación y Análisis Alimentarios,

23 c/ Constantino Candeira s/n, 15782, Santiago de Compostela (A Coruña), Spain; Tel:

24 34981563100; Fax: 34881816070; E-mail: josemanuel.leiro@usc.es

25 SUMMARY

26 Scuticociliatosis is a severe disease in farmed flatfish. However, the causative agent is
27 not always accurately identified. In this study, we identified two isolates of
28 scuticociliates from an outbreak in cultured fine flounder *Paralichthys adspersus*.
29 Scuticociliate identification was based on morphological data, examination of life stages
30 and the use of molecular approaches. The isolates were compared with a strain of
31 *Philasterides dicentrarchi* from turbot *Scophthalmus maximus* and with a strain
32 deposited in the American Type Culture Collection as *Miamiensis avidus* ATCC[®]
33 50180[™]. The use of morphological, biological, and molecular methods enabled us to
34 identify the isolates from the fine flounder as *P. dicentrarchi*. Comparison of *P.*
35 *dicentrarchi* isolates and *M. avidus* revealed some differences in the buccal apparatus.
36 Unlike *P. dicentrarchi*, *M. avidus* has a life cycle with three forms: macrostomes
37 (capable of feeding on *P. dicentrarchi*), microstomes, and tomites. Additionally, we
38 found differences in the 18S rRNA and α - and β -tubulin gene sequences, indicating that
39 *P. dicentrarchi* and *M. avidus* are different species. We therefore reject the synonymy /
40 conspecificity of the two taxa previously suggested. Finally, we suggest that a
41 combination of morphological, biological, molecular (by multigene analysis), and
42 serological techniques could improve the identification of scuticociliates parasites in
43 fish.

44

45 Key words:

46 *Paralichthys adspersus*; *Scophthalmus maximus*; scuticociliates; SSUrRNA gene; α - β -
47 tubulin gene.

48

49

50 INTRODUCTION

51 Scuticociliatosis is a parasitic disease caused by around 20 species of ciliates
52 included in the subclass Scuticociliatia Small, 1967. The ciliates are common free-living
53 members of limnetic and marine ecosystems and can transform into histiophagous
54 parasites that cause serious infections in some aquatic animals (Kim *et al.* 2004a;
55 Harikrishnan *et al.* 2010; Fan *et al.* 2011; Pan *et al.* 2013). Scuticociliates can infect a
56 wide variety of teleost fish species: the European seabass *Dicentrarchus labrax*
57 (Linnaeus, 1758) (Dragesco *et al.* 1995; Ramos *et al.* 2007); the Southern bluefin tuna
58 *Thunnus maccoyii* (Castelnau, 1872) (Munday *et al.* 1997); the silver pomfret *Pampus*
59 *argenteus* (Euphrasen, 1788) (Azad *et al.* 2007); the black rockfish *Sebastes schlegelii*
60 Hilgendorf, 1880 (Whang *et al.* 2013); hatchery-reared juveniles of the Hapuku
61 wreckfish *Polyprion oxygeneios* (Schneider & Forster, 1801) and adult kingfish *Seriola*
62 *lalandi* Valenciennes, 1833 (Smith *et al.* 2009); the sea dragons *Phyllopteryx*
63 *taeniolatus* (Lacepède, 1804) and *Phycodurus eques* (Günther, 1865) (Umehara *et al.*
64 2003; Rossteuscher *et al.* 2008; Bonar *et al.* 2013); the seahorses *Hippocampus erectus*
65 Perry, 1810, *H. kuda* Bleeker, 1852, *H. abdominalis* Lesson, 1872, and *H. hippocampus*
66 (Linnaeus, 1758) (Thompson & Moewus 1964; Shin *et al.* 2011; di Cicco *et al.* 2013;
67 Declercq *et al.* 2014; Ofelio *et al.* 2014); and elasmobranch fish such as the zebra shark
68 *Stegostoma fasciatum* Hermann, 1783, the shark of Port Jackson *Heterodontus*
69 *portusjacksoni* Meyer, 1793, and the Japanese bullhead shark *H. japonicus* Micklouho-
70 MaClay and MacLeay, 1884 (Stidworthy *et al.* 2014). Scuticociliates also can colonize
71 crustaceans and echinoderms, acting either as parasites or commensals (Small *et al.*
72 2005; Lynn & Strüder-Kypke 2005). One of the major problems in diagnosing fish
73 scuticociliatosis is the difficulty in identifying the pathogenic species causing the
74 disease. Although morphological and morphogenetic characters of the ciliary pattern

75 are routinely identified by using various silver impregnation methods, the systematic
76 positions of certain taxa remain ambiguous and their characteristics must be reviewed so
77 that species can be correctly identified (Jung *et al.* 2005; Miao *et al.* 2008; Gao *et al.*
78 2013). Biochemical, molecular, and immunological techniques must be accompanied by
79 conventional morphological studies based on light microscopic analyses of live and
80 silver-stained material for the correct identification of scuticociliate species, as well as
81 for the reconstruction of the phylogenetic relationships and the analysis of the
82 intraspecific variation between strains (Budiño *et al.* 2011a, 2012; Pan *et al.* 2013).

83 Many scuticociliates, especially species of the genera *Pseudocohnilembus* Evans
84 and Thompson, 1964, *Uronema* Dujardin, 1841, *Miamiensis* Thompson and Moewus,
85 1964, and *Philasterides* Kahl, 1926, have been associated with infections in flatfish.
86 Such infections seriously affect culture of the turbot *Scophthalmus maximus* (Linnaeus,
87 1758) and the olive flounder *Paralichthys olivaceus* (Temminck & Schlegel, 1846),
88 causing high mortalities and economic losses on fish farms (Iglesias *et al.* 2001; Kim *et*
89 *al.* 2004a). *Philasterides dicentrarchi* Dragesco, Dragesco, Coste, Gasc, Romestand,
90 Raymond and Bouix, 1995 has been identified as the main aetiological agent of
91 scuticociliatosis in farmed turbot and olive flounder on the basis of morphological and
92 molecular criteria (Iglesias *et al.* 2001; Paramá *et al.* 2006; Kim *et al.* 2004a). Recently,
93 Jung *et al.* (2005) identified several specimens isolated from the olive flounder as
94 *Miamiensis avidus* Thompson & Moewus, 1964, on the basis of morphological criteria.
95 Synonymy between these ciliate species was suggested after comparison of the
96 morphological characteristics and the SSUrRNA gene sequences of *M. avidus* and *P.*
97 *dicentrarchi* isolates (Jung *et al.* 2007). Hence, *P. dicentrarchi* is considered a junior
98 synonym of *M. avidus* (Song & Wilbert 2000; Jung *et al.* 2007; Song *et al.* 2009a; Gao
99 *et al.* 2010; Budiño *et al.* 2011a).

100 To date, identification and characterization of the species responsible for most
101 outbreaks of scuticociliatosis in turbot and olive flounder have been based on the
102 original morphological descriptions of *P. dicentrarchi* (Dragesco *et al.* 1995) and *M.*
103 *avidus* (Thompson & Moewus, 1964), or on available data on nucleotide sequences of
104 ribosomal genes obtained by different authors in various ciliate strains isolated from
105 turbot (Paramá *et al.* 2006) and from olive flounder (Jung *et al.* 2011). However,
106 identification has never been made by comparing the nucleotide sequences of the
107 species *M. avidus* currently deposited in ATCC (*M. avidus* ATCC[®] 50180[™]). This
108 restricts the accurate identification of this species at the molecular level.

109 In this study, we (i) describe an outbreak of scuticociliatosis in fine flounder
110 *Paralichthys adspersus* (Steindachner, 1867) cultured in Peru and (ii) compare the
111 morphological and biometrical characteristics, SSUrRNA, α - and β -tubulin gene
112 sequences, antigenic relationships, tomitogenesis, and prey induced transformation in
113 ciliates isolated from the fine flounder, in the ciliate *P. dicentrarchi* isolated from turbot,
114 and in the ciliate species *M. avidus* ATCC[®] 50180[™] (strain Ma/2). The results provide
115 new data that should be considered in the identification of the aetiological agents of
116 scuticociliatosis in flatfish.

117

118 MATERIAL AND METHODS

119 *Animals and ethical approval*

120 Twenty specimens of turbot *Scophthalmus maximus* of approximately 50 g body
121 weight were obtained from a local fish farm (Galicia, NW Spain). The fish were
122 maintained in 50-l closed-circuit aerated tanks at 17-18 °C. Ten ICR (Swiss) CD-1 mice
123 (between eight and ten weeks old) initially supplied by the Charles River Laboratories
124 (USA) were bred and maintained in the Central Animal Facility of the University of

125 Santiago de Compostela (Spain). The mice were held according to the criteria of
126 protection, control, care and welfare of animals and the legislative requirements relating
127 to the use of animals for experimentation (EU Directive 86/609 / EEC), the Declaration
128 of Helsinki, and/or the Guide for the Care and Use of Laboratory Animals as adopted
129 and promulgated by the US National Institutes of Health (NIH Publication No. 85-23,
130 revised 1996). The Institutional Animal Care and Use Committee of the University of
131 Santiago de Compostela approved all experimental protocols.

132

133 *Isolation, ciliate culture, and experimental infections*

134 In 2014, an outbreak of scuticociliatosis affecting the fine flounder *P. adspersus* was
135 detected on a fish farm in Peru (Ancash, Huarney Province). The farm was equipped
136 with two water flow systems: one with closed and the other with open recirculation.
137 Mortality was very high in both systems, affecting fish of different sizes. Outbreaks of
138 scuticociliatosis in fine flounder coincided with a series of anomalies in the seawater
139 temperature registered in the eastern Pacific region affected by El Niño resulting in an
140 average temperature that was 3.1 °C higher than the annual average (Comunicado
141 Oficial ENFEN – Estudio Nacional del Fenómeno El Niño-N°09-2014, Instituto del Mar
142 del Perú –IMARPE). Ciliates were isolated from fish ranging from 16-27 cm in size
143 (Fig. 1A). Two isolates of the scuticociliates, denominated Pe5 and Pe7, were obtained
144 from ascitic fluid (with a concentration of approximately 5×10^6 trophozoites /ml) of
145 naturally infected specimens of the fine flounder *P. adspersus*.

146 Virulent strain I1 of *P. dicentrarchi* was originally isolated from ascites fluid
147 turbot from infected fish on a farm in Galicia (NW Spain) (Iglesias *et al.* 2001).

148 Strain Ma/2 of *M. avidus* deposited by A.T. Soldo and E. B. Small (Veterans
149 Administration Medical Center, Miami, FL) with the name *Miamiensis avidus*

150 Thompson and Moewus (ATCC[®] 50180TM) was acquired from the American Type
151 Culture Collection (ATCC, USA). The strain Ma/2 of *M. avidus* belonged to the
152 collection of Dr G.G. Holz and it was originally isolated by Dr L Moewus from infected
153 seahorses and cultivated axenically since 1963 (Moewus, 1963; Kaneshiro *et al.* 1969).

154 Isolates Pe5, Pe7, and *P. dicentrarchi* strain I1 were maintained in the laboratory
155 under the culture conditions described by Iglesias *et al.* (2003a). Strain Ma/2 of *M.*
156 *avidus* was cultivated axenically in ATCC[®] medium 1651 MA (LGC Standards, Spain)
157 at 25 °C and subcultured every 3-5 days.

158 For experimental infections, turbot were injected intraperitoneally with 0.1 ml of
159 10⁶ ciliates/ml (*M. avidus*, strain Ma/2) in phosphate-buffered saline (PBS) containing
160 10 mM Na₂HPO₄, 2mM KH₂PO₄, 2.7 mM KCl, and 137 mM NaCl, as previously
161 described (Paramá *et al.* 2003), and the fish were observed daily for signs of infection
162 and mortality. Infection was confirmed *post mortem* by the presence of ciliates in
163 organs and tissues.

165 *Morphological and histological analyses*

166 Ciliates obtained at the exponential phase of culture (days 2-3) were concentrated by
167 centrifugation at 700 g for 5 min and stained by a modification of the amoniactal silver
168 carbonate method originally described by Fernández-Galiano (1994) and described in
169 detail by Budiño *et al.* (2011a).

170 The nuclear apparatus was visualized by fluorescence, after staining ciliates with
171 an aqueous solution of 0.4 µg/ml of 4'-6-diamidine-2-phenylindone (DAPI, Sigma-
172 Aldrich), in a Zeiss Axioplan microscope (Jena, Germany) equipped with a DAPI filter
173 set (BP 365/12; FT 395; LP 397) and in a Leica TCS SP2 laser scanning confocal
174 microscope (Leica Biosystems, Mannheim, Germany).

175 Somatic and caudal cilia were measured in parasites fixed in 10% buffered
176 formaldehyde under phase contrast optics.

177 In some experiments of prey-induction transformation, the ciliates were stained
178 with the pH sensitive fluorescent acridine orange and observed in a fluorescence
179 microscope with an excitation BP 450/490 nm dichroic mirror filter and FT 510 nm LP
180 emission filter.

181 For histological study, tissues were fixed in 10% buffered formaldehyde solution,
182 dehydrated through an ethanol series, embedded in Paraplast Plus (Sigma-Aldrich),
183 sectioned at 2-5 μm with a Leica RM 2135 rotary microtome (Leica Biosystems,
184 Germany), and stained with haematoxylin and eosin (H&E) for examination by light
185 microscopy (Iglesias *et al.* 2001).

186

187 *Tomitogenesis and prey induction experiments*

188 For tomite transformation, cultures of 2×10^3 cells/ml of *M. avidus* strain Ma/2, *P.*
189 *dicentrarchi* strain I1 and isolate Pe5 in stationary phase were centrifuged at 700 g for 5
190 min, resuspended in non-nutrient synthetic seawater (NSS, 8 ‰ salinity), and incubated
191 at 25 °C (Gómez-Saladín & Small, 1993a). In prey induction experiments, ciliates of *M.*
192 *avidus* strain Ma/2 and *P. dicentrarchi* strain I1 were incubated at a ratio of 1:1 in 24-
193 well microplates for 5 days in NSS at 25 °C. The ciliates were observed daily under an
194 inverted optical microscope. When predation phenomena were observed, ciliates were
195 removed and centrifuged at 700 g for 5 min. Some specimens (10^6 ciliates) were fixed
196 in buffered 10% formaldehyde in phosphate buffer saline for later examination by phase
197 contrast microscopy, while other specimens (10^6 ciliates) were stained, using a
198 modification of the ammoniacal silver carbonate method, as described previously.

199

200 *PCR, cloning, and phylogenetic analyses*

201 Cultured ciliates (5×10^6 cells/ml) were harvested by centrifugation at 700 g for 5 min.
202 The ciliates were washed twice with phosphate buffer saline (PBS) and total DNA was
203 purified with DNAeasy Blood and Tissue Kit (Qiagen) according to the manufacturer's
204 instructions. DNA was analyzed to estimate its quality, purity, and concentration by an
205 A_{260} measurement in a NanoDrop ND-1000 Spectrophotometer (NanoDrop
206 Technologies, USA.). The DNA was stored at -20°C until use.

207 PCR amplification was performed as previously described (Leiro *et al.* 2000;
208 Budiño *et al.* 2011a), with minor modifications. A complete small-subunit ribosomal
209 RNA (SSUrRNA; 1,759 bp), a region of 388 bp of the gene coding the β -tubulin, and a
210 region of 197 bp of the gene coding the α -tubulin were amplified. The primer sets were
211 designed and optimized by use of the Primer 3Plus program
212 (<http://www.bioinformatics.nl/cgi-bin/primer3plus/primer3plus.cgi>), with default
213 parameters. The PCR mixtures (25 μl) contained PCR reaction buffer (10 mM Tris-HCl,
214 50 mM KCl, 1.5 mM MgCl_2 , pH 9.0), 0.2 mM of each deoxynucleoside triphosphate
215 (dNTPs, Roche), 0.4 μM of each primer [forward 5'-
216 AATCTGGTTGATCCTGCCAGT-3' / reverse 5'-GATCCTTCCGCAGGTTCA-3'
217 (SSUrRNA); forward 5'-CCTACCACGGAGACTCTGATT-3' / reverse 5'-
218 CCATAATTCTGTCGGGGTATT-3' (β -tubulin); forward 5'-
219 ATGCCCTCTGATAAAACCATC-3' / reverse 5'-GAGTCCGGTACAGTTGTCAG-3'
220 (α -tubulin)]; 0.5 units of high fidelity Taq polymerase (Nzyproof DNA polymerase;
221 Nzytech, Portugal) and 50 ng of genomic DNA. The reactions were run in an automatic
222 thermocycler (iCycler, BioRad, USA) as follows: initial denaturing at 94°C for 5 min,
223 followed by 35 cycles at 94°C for 30 s, annealing at 55, 57, and 64°C (for SSUrRNA,
224 α -tubulin and β -tubulin, respectively) for 45 s, and 72°C for 1 min; and finally a 7 min

225 extension phase at 72 °C. The PCR products were analysed on a 4% agarose gel in tris
226 acetate ethylenediaminetetraacetic acid (TAE) buffer (40 mM Tris–acetate, pH 8.0, 2
227 mM EDTA) containing Sybr Green at 1x concentration (Intron, Korea), to verify the
228 presence of bands of the correct size, and were photographed with a digital camera. The
229 PCR products were cloned in the pSpark® II DNA cloning vector kit (Canvax Biotech,
230 Spain) according to the manufacturer's instructions. After ligation of the PCR fragment,
231 the *E. coli* DH_{5α} cells were transformed and then selected on the basis of antibiotic
232 sensitivity and colour by culture on LB agar plates containing 100 µg/ml ampicillin,
233 with 50 µl of a stock solution of 20 mg/ml of 5-bromo-4-chloro-3-indolyl-β-galactoside
234 (X-Gal) and 20 µl of a 0.5 M solution of isopropylthio-β-D-galactoside (IPTG) spread
235 on the surface. Ten *E. coli* white colonies per ligation sample were amplified in LB
236 medium and plasmid DNA was purified with the QiAprep® Spin Miniprep kit (Qiagen,
237 Germany) according to the manufacturer's instructions. To confirm the presence of the
238 cloned fragment of the correct size, the fragment was amplified by PCR, with the
239 previously indicated primers and conditions. The PCR-amplified products were then
240 visualized by agarose gel electrophoresis and sequenced in complementary directions
241 (Sistemas Genómicos, Spain).

242 We used the BLAST interface and the blastn program optimized for very similar
243 sequences (megablast), available at <http://blast.ncbi.nlm.nih.gov>, to calculate the degree
244 of identity between the nucleotide sequences. Sequence alignment can be performed
245 directly online.

246 The complete nucleotide sequences of the SSUrRNA gene from isolates Pe5 and
247 Pe7 from fine flounder, strain I1 of *P. dicentrarchi* isolated from turbot, and strain Ma/2
248 of *M. avidus* (ATCC® 50180™) were compared with equivalent sequences from strains
249 YK2 and YS2 of *M. avidus* isolated from olive flounder (accession numbers EU831208

250 and EU831200; Jung *et al.*, 2011) and with other species of the order Philasterida
 251 (Table 1). The sequences were aligned with Clustal Omega (McWilliam *et al.*, 2013)
 252 and phylogenetic trees were inferred by the neighbour-joining (NJ) method (Saitou &
 253 Nei, 1987). This method was applied to the Kimura two-parameter correction model
 254 (Kimura, 1980) by bootstrapping with 1,000 replicates (Felsenstein, 1985) from
 255 multiple alignments and consensus of the study sequences with Clustal Omega software
 256 (Sievers *et al.* 2011). The tree is drawn to scale, with branch lengths in the same units as
 257 those of the evolutionary distances used to infer the phylogenetic tree. All positions
 258 containing gaps and missing data were eliminated and evolutionary analyses were
 259 conducted in MEGA7 (Kumar *et al.* 2016)

260

261 *Production of recombinant alpha-tubulin ($r\text{-}\alpha\text{Tub}$) of *P. dicentrarchi* in*
 262 *yeast cells*

263 RNA isolated from *Philasterides dicentrarchi* was purified with a NucleoSpin RNA kit
 264 (Macherey-Nagel, Düren, Germany) according to the manufacturer's instructions. After
 265 purification of the RNA, the quality, purity, and concentration were measured in a
 266 NanoDrop ND-1000 Spectrophotometer (NanoDrop Technologies, USA). The reaction
 267 mixture used for cDNA synthesis (25 μl /reaction mixture) contained 1.25 μM random
 268 hexamer primers (Promega), 250 μM of each deoxynucleoside triphosphate (dNTP), 10
 269 mM dithiothreitol (DTT), 20 U of RNase inhibitor, 2.5 mM MgCl_2 , 200 U of MMLV
 270 (Moloney murine leukemia virus reverse transcriptase; Promega) in 30 mM Tris and 20
 271 mM KCl (pH 8.3), and 2 μg of sample RNA. The PCR was carried out with gene-
 272 specific primers designed from a partial sequence of the α -tubulin of *P. dicentrarchi*

273 (forward/reverse primer pair 5'-

274 AAAGAAGAAGGGGTACCTTTGGATAAAAGAatgcctctgataaaaccatc-3' / 5'-

275 TGGGACGCTCGACGGATCAGCGGCCGCTTAGTGGTGGTGGTGGTGGTggagtc
276 cggtagcagttgtcag-3'). These primers were designed and optimized, using the
277 *Saccharomyces* Genome Database (<http://www.yeastgenome.org/>). A hybridization
278 region with the yeast YEpFLAG-1 (Eastman Kodak Company) plasmid and a poly His
279 region (lower case letters correspond with the gene annealing zone) were included. The
280 PCR reaction was initially developed at 95 °C for 5 min, and then for 30 cycles of 94 °C
281 for 1 min, 53 °C for 1.5 min and 72 °C for 2 min. At the end of the 30 cycles, a 7-min
282 extension phase was carried out at 72 °C. The PCR products were purified by using the
283 Gene Jet PCR Purification Kit (Fermentas, Life Sciences) according to the
284 manufacturer's instructions.

285 Purified PCR products were cloned in YEpFLAG-1 (Eastman Kodak Company)
286 yeast expression vector, a plasmid carrying a TRP1 gene that completes the auxotrophy
287 for the tryptophan for the host yeast (López-López *et al.* 2010).

288 Linearized plasmid YEpFLAG-1 was digested with *EcoRI* and *Sall* (Takara) and
289 used to transform *Saccharomyces cerevisiae* cells (strain BJ 3505) by the lithium
290 acetate procedure (Ito *et al.* 1983). The procedure involves co-transformation of yeast
291 cells with the linearized empty plasmid and the PCR-generated DNA fragment, so that a
292 recombination process occurs within the cell to yield a plasmid bearing the desired
293 insert. Positive colonies were selected on complete medium containing glucose (20 g/l),
294 but without tryptophan (CM-Trp), Yeast Nitrogen Base medium without amino acids
295 (Sigma-Aldrich), except for the amino acids arginine, methionine and threonine at 10
296 mg/l; adenine, histidine, leucine, lysine, and tyrosine at 40 mg/l; and isoleucine and
297 phenylalanine at 60 mg/l.

298 Plasmid DNA was then extracted with Easy Yeast Plasmid Isolation Kit
299 (Clontech) according to the manufacturer's instructions. The purified and cloned DNA
300 fragment was subjected to sequencing analysis (Sistemas Genómicos, Spain).

301

302 *Inoculation and polyclonal mouse antisera*

303 CD-1 mice were inoculated i.p. with 200 μ l of a 1:1 emulsion composed of 100 μ l of a
304 solution of 100 μ g of r- α Tub of the strain I1 of *P. dicentrarchi* in PBS and 100 μ l of
305 Freund complete adjuvant (Sigma-Aldrich). The same dose of r- α Tub protein was
306 prepared in Freund's incomplete adjuvant and injected i.p. in mice 15 and 30 days after
307 the first immunization. The mice were bled via retrobulbar venous plexus seven days
308 after the second inoculation. The blood was left to coagulate overnight at 4 °C before
309 the serum was separated by centrifugation (2000 g for 10 min), mixed 1:1 with glycerol,
310 and stored at -20 °C until use (Piazzon *et al.* 2011).

311

312 *Immunoassays*

313 For Western-blot assay, integral ciliate membrane-associate proteins (CMP) of
314 scuticociliates were prepared as previously described (Iglesias *et al.* 2003b), with minor
315 modifications (Mallo *et al.* 2013). Briefly, scuticociliate trophozoites were deciliated by
316 the method described by Dickerson *et al.* (1989). The integral proteins were extracted
317 by phase separation in Triton X-114 solution according to the method described by
318 Bordier (1981). The proteins were precipitated with cold acetone, and the precipitate was
319 dried in a Speed Vac concentrator and stored at -80 °C in 10 mM Tris-HCl, pH 7.5.
320 Samples from CMP were separated under non-reducing conditions on linear SDS-
321 PAGE 12.5 % gels (Piazzon *et al.* 2008). On completion of the electrophoresis, the gels
322 were stained with Thermo Scientific GelCode Blue Safe Protein Stain (Thermo Fisher,

323 USA) for qualitative determination of the protein bands. At the same time, a gel was
324 immunoblotted at 15 V for 35 min to Immobilon-P transfer membranes (0.45 μm ;
325 Millipore, USA) in a trans-blot SD transfer cell (Bio-Rad, USA) with transference
326 buffer (48 mM Tris, 29 mM glycine, 0.037% SDS and 20% methanol, pH 9.2). The
327 membrane was washed with Tris buffer saline (TBS; 50 mM Tris, 0.15 M NaCl, pH
328 7.4) and immediately stained with Ponceau S to verify transfer. After destaining the
329 membrane with bidistilled water, a blocking solution consisting of TBS containing 0.2%
330 Tween 20 and 3% BSA was added. The membrane was incubated for 1.5 h at room
331 temperature and then washed in TBS and incubated overnight with the mouse
332 polyclonal antisera anti-r- αTub (1:500 dilution) at 4 °C. The membrane was washed
333 again with TBS and incubated with rabbit anti-mouse IgG (Dakopatts; dilution 1:6000)
334 for 1 h at room temperature. The membrane was then washed five times for 5 min with
335 TBS and incubated for 1 min with enhanced luminol-based chemiluminiscent substrate
336 (Pierce ECL Western Blotting Substrate, Thermo Scientific, USA), before finally being
337 visualized and photographed with a FlourChem® FC2 imaging system (Alpha Innotech,
338 USA).

339 The immunofluorescence assay was performed according to the previously
340 described protocol (Mallo *et al.* 2015, 2016). Briefly, 5×10^6 ciliates were centrifuged
341 at 750 *g* for 5 min, washed twice with Dulbecco's phosphate buffered saline (DPBS,
342 Sigma Aldrich) and fixed for 5 min in a solution of 4% formaldehyde in DPBS. The
343 ciliates were then washed twice with DPBS, resuspended in a solution containing 0.1%
344 Triton X-100 (PBT) for 3 min and then washed twice with DPBS. They were then
345 incubated with 1% bovine serum albumin (BSA) for 30 min. After this blocking step,
346 the ciliates were incubated at 4 °C overnight with a solution containing a 1:100 dilution
347 of anti-r- αTub . The ciliates were then washed three times with DPBS and incubated, for

348 1 h at room temperature, with a 1:100 dilution of FITC conjugated rabbit/goat anti-
349 mouse IgG-FITC antibody (Sigma) or with the same dilution of Alexa Fluor 546
350 conjugated goat anti-mouse Ig (Molecular Probes). After three washing steps in DPBS,
351 the samples were double-stained with 0.8 mg/ml 4', 6-diamidino-2-phenylindole (DAPI;
352 Sigma-Aldrich) in DPBS for 15 min at room temperature (Paramá *et al.* 2007). After
353 another three washing steps in DPBS, the samples were mounted in PBS-glycerol (1:1)
354 and visualized by fluorescence microscopy (Zeiss Axioplan, Germany) and/or confocal
355 microscopy (Leica TCS-SP2, LEICA Microsystems Heidelberg GmbH, Mannheim,
356 Germany).

357 The enzyme-linked immunosorbent assay (ELISA) was performed as previously
358 described (Iglesias *et al.* 2003b), with minor modifications. One µg of CMP in 100 µl of
359 carbonate-bicarbonate buffer (pH 9.6) was added to 96-well ELISA plates (high binding,
360 Greiner Bio-One, Germany) and incubated overnight at 4 °C. The wells were then
361 washed three times with TBS and blocked for 1 h with TBS containing 0.2% Tween 20
362 (TBS-T₁) and 5% non-fat dry milk. The plates were incubated for 30 min at room
363 temperature in a microplate shaker for ELISA (Stuart, UK) at 750 rpm with a 1:100
364 dilution (in TBS-T₁ containing 1% non-fat dry milk) of anti-r-αTub, and washed five
365 times with TBS containing 0.05% Tween 20. Bound mouse antibodies were detected
366 with a peroxidase-conjugated anti-mouse Ig polyclonal rabbit serum (DAKO) diluted
367 1:1000 in TBS-T₁, and incubated for 30 min with shaking. The plates were washed five
368 times in TBS, and 100 µl of *o*-phenylenediamine dihydrochloride (OPD, Sigma-
369 Aldrich) and 0.003% H₂O₂ were added to each well. After incubation of the plates for
370 20 min at room temperature in darkness, the enzymatic reaction was stopped by adding
371 25 µl of H₂SO₄ at 3 N. Finally, the absorbance was read at 492 nm in a
372 spectrophotometer microplate reader (Bio-Tek Instruments, USA).

373 *Statistical analysis*

374 Results are expressed as means \pm standard error of means. Data were tested by one-way
375 analysis of variance (ANOVA) followed by a Tukey-Kramer test for multiple
376 comparisons. Differences were considered significant at $P < 0.05$.

377

378 RESULTS

379

380 *Description of an outbreak of scuticociliatosis in the fine flounder*

381 *Paralichthys adspersus*

382 The outbreak of scuticociliatosis coincided with water temperatures higher than
383 21-22 °C. The main external symptoms of the affected fish were alterations in skin
384 pigmentation and emaciation (Fig. 1A), gills congested with mucus and abundant
385 aneurysms (Fig. 1B, D), exophthalmia, and abdominal distension with ascitic fluid,
386 from which ciliates were isolated (Fig. 1C). At the histopathological level, the main
387 pathology was associated with systemic necrosis affecting several organs including the
388 heart, with severe necrosis of myocardium (Fig. 1D).

389

390 *Description of the Peruvian population (isolates Pe5 and Pe7) infecting the*

391 *fine flounder P. adspersus (Fig. 2A-I; Table 2)*

392 The main characteristics of the ciliates isolated from the fine flounder are as
393 follows: cells elongated and spindle-shaped, with a pointed anterior and rounded
394 posterior end, a contractile vacuole, and a prominent caudal cilium (Fig. 2B, E, G, I,
395 3C). The buccal apparatus always contained two paroral membranes (PM1 and PM2)
396 and three oral membranoids or polykinetids (M1, M2, and M3) (Fig. 2A, D, F, H),

397 showing identical morphology to that of *Philasterides dicentrarchi* (Fig. 2C). PM1
398 extends from the start of M1 to the start of M3, while PM2 extends from the middle of
399 M3 to the end of the oral cavity (Fig. 2A, C, D, F, H). M1 is elliptical, M2 is trapezoidal,
400 and M3 is smaller than M1 and M2, and irregularly triangular (Fig. 2A, C, D, F, H). The
401 somatic ciliature of the Pe5 and Pe7 isolates consists of 10-13 kineties, and the pore of
402 the subterminal contractile vacuole is at the posterior end of the second kinety (Fig. 2B,
403 E, G, I).

404 The morphometric data of the Pe5 and Pe7 isolates are summarized in Table 2,
405 in which they are compared with the morphometric data available for *P. dicentrarchi*
406 isolated from turbot (strain I1; present study) and from seabass (Dragesco *et al.* 1995),
407 and for *M. avidus* isolated from seahorses (Thompson & Moevus 1964) as well as with
408 own data from of strain Ma/2 of *Miamiensis avidus* Thompson & Moewus
409 (ATCC[®] 50180[™]) stained with ammoniacal silver carbonate and *P. dicentrarchi* strain
410 I1. The ranges of the morphological data on isolates Pe5 and Pe7 generally overlap
411 those of *P. dicentrarchi* strain I1, of the original species description of *M. avidus*, and of
412 *M. avidus* held by the ATCC. At the morphological level, isolates Pe5 and Pe7 and *P.*
413 *dicentrarchi* strain I1 differ several morphological features from *M. avidus* (ATCC),
414 such as the lack of a peak at the frontal part of trophozoites (Fig. 2M), the lack of a
415 continuous paroral membrane (PM; Fig. 2J, K, L), and the morphology of the tomites,
416 which are elongated and fusiforms in the latter species (Fig. 2N, O). In contrast to *M.*
417 *avidus* (ATCC), the *P. adspersus* isolates Pe5 and Pe7 as well as *P. dicentrarchi* have a
418 prominent caudal cilium that is longer than the somatic cilia (Fig. 3C). In *P.*
419 *dicentrarchi*, the mean length of the caudal cilium was $11.4 \pm 2.0 \mu\text{m}$ (15 μm) and of
420 the somatic cilia was $5.6 \pm 1.0 \mu\text{m}$ (5-8 μm). In *M. avidus* strain Ma/2, the mean

421 length of the caudal cilium was $9.3 \pm 2.1 \mu\text{m}$ (7-11 μm) and that of the somatic cilia,
422 $6.6 \pm 1.1 \mu\text{m}$ (5-9 μm , n=20).

423 The nuclear apparatus of isolates Pe5 and Pe7 and strain I1 of *P. dicentrarchi*
424 consists of a spherical macronucleus located mainly in the middle or anterior third of
425 the trophozoite, slightly lateralized, and between 4-8 μm in diameter (Table 2; Fig. 3A-
426 C). The micronucleus, 1-2 μm in diameter, has a variable posterior position in isolates
427 Pe5 and Pe7 and strain I1 of *P. dicentrarchi* (Fig. 3A-C), (Table 2). In *M. avidus* strain
428 Ma/2, the macronucleus is irregularly spherical and usually located in the anterior cell
429 half. The micronucleus anterior or laterally of the macronucleus (Fig. 3D).

430

431 *Tomitogenesis and predatory transformation*

432 Most polymorphic hymenostomes and scuticociliates have morphologically distinct
433 feeding stages including a bacteriovorus microstome, a predatory macrostome, and
434 sometimes a non-feeding, fast swimming tomite (Fig. 4). In culture media containing
435 nutrients, *M. avidus* strain Ma/2 produced macrostome and microstome forms (Fig. 4A),
436 while all strains of *P. dicentrarchi* only produced microstome forms (Fig. 4C). Under
437 conditions of nutrient deprivation, *M. avidus* Ma/2 produced some macrostome and
438 microstome forms and numerous tomites (Fig. 4B) *P. dicentrarchi* appeared almost
439 exclusively as tomites (Fig. 4D). In *M. avidus* strain Ma/2, the macrostomes measured
440 $50.1 \pm 9.4 \times 35.4 \pm 5.2 \mu\text{m}$ (37-65 \times 28-44 μm , n= 10) and the tomites $22.4 \pm 4.5 \times$
441 $10.5 \pm 2.7 \mu\text{m}$ (23-28 \times 7-13 μm , n= 10). In *P. dicentrarchi*, the length/width of the
442 tomite was $20.6 \pm 2.7 \times 13.1 \pm 2.1$ (17-24 \times 11-16 μm , n= 10).

443 To verify which of the species considered in this study developed predatory
444 macrostome phases, we co-cultured trophozoites of *M. avidus* strain Ma/2 with
445 trophozoites of *P. dicentrarchi* strain I1, and trophozoites of strain I1 with isolate Pe7,

446 in media without nutrients. On the second day, the co-cultures of *M. avidus* strain Ma/2
447 and *P. dicentrarchi* strain I1 showed predatory macrostome forms (Fig. 5A-D); however,
448 this phenomenon was not detected in the co-cultures of Pe7 and I1 isolates. We found
449 that *M. avidus* is a predator of *P. dicentrarchi* strain I1. To reach this conclusion, we
450 obtained genomic DNA from *M. avidus* and *P. dicentrarchi* from 5 day co-cultures at
451 day 5 and amplified it by PCR (Fig. 5E), using the primers designed for *P. dicentrarchi*
452 DNA genes and showing low (α -tubulin), very low (β -tubulin) and high (SSUrRNA)
453 nucleotide identity with the same genes in *M. avidus* (Fig. 5F). In all cases, we observed
454 amplification of the SSUrRNA gene, slight amplification of the α -tubulin gene, and
455 non-amplification of the β -tubulin gene in DNA samples obtained from cultures of the
456 strain Ma/2 of *M. avidus* and in DNA samples from co-cultures of *M. avidus* and *P.*
457 *dicentrarchi* (Fig. 5E, a-c). We then cloned and sequenced the amplified fragments of
458 α -tubulin and SSUrRNA genes from co-cultures of *M. avidus* strain Ma/2 and *P.*
459 *dicentrarchi* strain I1, observing that the nucleotide sequence obtained coincided with
460 those of *M. avidus* Ma/2 (Fig. 5E, a, c).

461

462 *Infectivity of M. avidus strain Ma/2*

463 The *M. avidus* strain ATCC[®] 50180[™] was originally isolated from infected
464 seahorses; however, we did not know whether the species could infect flatfish. In this
465 experiment, we inoculated turbot by intraperitoneal injection with *M. avidus*, using the
466 same dose as used for *P. dicentrarchi* strain I1 (10^5 ciliates/fish). We observed that *M.*
467 *avidus* strain Ma/2 is highly pathogenic to turbot, generating abdominal distension with
468 a significant presence of ascitic liquid, from which it was possible to isolate ciliates (Fig.
469 6A), and causing 100% mortality in infected fish on day 5 (Fig. 6B).

470

471 *Molecular analysis of the scuticociliates*

472 The full length SSUrRNA sequences of Pe5, Pe7, and *P. dicentrarchi* strain I1
473 (Accession n° JX914665.1; Leiro *et al.* 2012, unpublished) showed 100% identity with
474 each other and 96% identity with *M. avidus* strain Ma/2 (Accession KX357144; Table
475 3A). We compared the above- mentioned 18S sequences with those obtained from the
476 GenBank for *M. avidus* isolate YK2 (Accession n° EU831208.1; Jung *et al.* 2011), *M.*
477 *avidus* isolate YS2 (Accession EU831200.1; Jung *et al.* 2011), *M. avidus* isolate
478 FXP2009050602 (Accession JN885091.1; Gao *et al.* 2012), and strain GF2008082801
479 of *Philasterides armatalis* Song, 2000 (Accession FJ848877; Gao *et al.* 2009).
480 *Miamiensis avidus* strains YK2 and YS2 showed 99% identity with *P. dicentrarchi* strain
481 I1, Pe5 and Pe7 isolates, 96% identity with *M. avidus* strain Ma/2 or *M. avidus* isolate
482 FXP2009050602, and 95% identity with *P. armatalis* (Table 3A). The phylogenetic tree
483 constructed, using the Neighbour-joining (NJ) model grouped Pe5, Pe7, *P. dicentrarchi*
484 strain I1 in the same node and closely related to strains YK2, YS2 (Fig. 7A), while *M.*
485 *avidus* strain Ma/2 from ATCC and the *M. avidus* isolate FXP2009050602 grouped in a
486 different node together with the *Anophryoides haemophila* (Fig. 7A). Analysis of the
487 similarity between the nucleotide sequences corresponding to fragments of the α - (strain
488 I1, accession KX357145; strain Ma/2, accession KX357143) and β -tubulin genes (strain
489 I1, accession CQ342956.1; strain Ma/2 accession KX357147) revealed 99-100%
490 identity between isolates Pe5, Pe7 and strain I1, but only 89% identity for α -tubulin and
491 85% identity for β -tubulin with *M. avidus* strain Ma/2 or 81-83% of identity for α -
492 tubulin with *M. avidus* isolate FXP2009050602 (Table 3B). Phylogenetic trees
493 generated after alignments of the nucleotide sequences of the α - and β -tubulin genes for
494 the Pe5 and Pe7 isolates and I1 and the Ma/2 strains, using the model NJ, grouped Pe5,

495 Pe7 and I1 in one node and the *M. avidus* Ma/2 strain or isolate FXP2009050602 in a
496 different node (Fig 7B, C).

497

498 *Antigenic relationships between ciliates isolated from flatfish and M.*
499 *avidus strain Ma/2*

500 We generated a recombinant protein from a partial sequence of the gene
501 encoding this protein (r- α Tub) in *P. dicentrarchi* strain I1, to compare the antigenic
502 homology between the α -tubulin of the scuticociliates Pe5, Pe7, I1, and *M. avidus* strain
503 Ma/2 (ATCC[®] 50180TM) (Fig. 8A). The antibodies generated in mice following
504 inoculation with the recombinant protein were used to perform three immunoassays to
505 determine the level of cross-reactivity with this protein in the isolates/strains studied.

506 We first performed an immunofluorescence test to verify the level of recognition
507 by anti-r- α Tub antibodies on the Pe5 and Pe7 isolates and the I1 and Ma/2 strains. We
508 found that the antibodies recognised the α -tubulins in all four samples and, at the
509 concentrations used, we did not find any qualitative differences in the staining intensity
510 (Fig. 8B-E).

511 Quantitative immunoassays as ELISA revealed that the levels of recognition of
512 native ciliary proteins containing α -tubulin in the Pe7 isolate were similar to those
513 obtained with strain I1; however, these levels were significantly lower when antigens of
514 strain Ma/2 of *M. avidus* were used (Fig. 8F).

515 Western blot carried out under reducing conditions revealed two bands of about
516 50 and 60 kD in ciliary isolated fractions of isolate Pe7 and strain I1. However, no
517 bands were detected when antigens from *M. avidus* strain Ma/2 were included (Fig. 8G).

518

519

520 DISCUSSION

521 Here we describe a scuticociliate infection in the fine flounder *Paralichthys*
522 *adpersus*, cultivated in Peru. The infection occurred on a fish farm with a water
523 recirculation system, which appears to increase the risk of scuticociliatosis (Budiño et al.
524 2011b), and at high temperatures, another risk factor for development of this disease
525 (Iglesias *et al.* 2001; Moustafa *et al.* 2010).

526 We did not conduct a complete histopathological study of the scuticociliatosis in
527 *P. adpersus* and only observed that the clinical signs and pathology generated by the
528 ciliates are very similar to those produced in *Scophthalmus maximus* (Linnaeus, 1758)
529 and the olive flounder *Paralichthys olivaceus* (Temminck & Schlegel, 1846) (Iglesias *et*
530 *al.* 2001; Jung *et al.* 2007; Moustafa *et al.* 2010; Harikrishnan *et al.* 2012). Our research
531 primarily focused on the identification of the causative agent of the disease in *P.*
532 *adpersus*. In all samples, the buccal apparatus of the ciliate isolates Pe5 and Pe7 from
533 *P. adpersus* contained two paroral membranes (PM1 and PM2) and three oral
534 polykinetids (M1, M2 and M3), with identical arrangement and morphology to that
535 described for *Philasterides dicentrarchi* (Dragesco *et al.* 1995; Iglesias *et al.* 2001;
536 Budiño *et al.* 2011a). According to the redescription of the genus *Philasterides* Kahl,
537 1926 by Grolière (1980), the type species *Philasterides armata* has a split paroral
538 membrane and three equidistant adoral polykinetids (M1, M2, and M3). However, of the
539 two paroral membranes is debated as it is uncertain whether it represents a fixed
540 character that includes this species in the genus *Philasterides* or may show an
541 intraspecific variability and is thus not suitable for species identification (Jung *et al.*
542 2007).

543 Song & Wilbert (2000) redescribed *M. avidus*, using the dimorphic paroral
544 membrane with its monokinetidal anterior and its dikinetidal posterior part slightly

545 separated as its main morphological characteristic, thereby synonymizing *M. avidus*
546 and *P. dicentrarchi*. However, the morphological data of the present study clearly
547 shows that both isolates obtained from *P. adspersus* (isolates Pe5 and Pe7) have two
548 clearly separated paroral membranes, while *M. avidus* strain Ma/2 has invariably a
549 single continuous paroral membrane. The original description of *M. avidus* mentions
550 that a narrow gap “sometimes” appears between the anterior and posterior paroral
551 portions; however, this does not seem to be common in this species, as indicated by the
552 fact that the authors described the paroral as a unit, measuring its length from its
553 anterior to its posterior end until the anterior end (Thompson & Moewus, 1964). In
554 contrast to *M. avidus*, the presence of a bipartite paroral membrane (PM1 and PM2),
555 seems thus to be a constant morphological feature in *P. dicentrarchi* (Dragesco *et al.*
556 1995; Iglesias *et al.* 2001; Budiño *et al.* 2011a).

557 Jung *et al.* (2007) found that a scuticociliate isolate (YS1 strain) from olive
558 flounder, identified as *M. avidus*, has one or two paroral membranes and two or three
559 oral polykinetids, the authors concluded that the morphology of buccal structures
560 “cannot be used as a consistent key for identification of the species”. However
561 variability reported by Jung *et al.* (2007), might the result of a stomatogenic sequence in
562 the organelles membranoidogenesis, which is very common in several species of
563 scuticociliates (Miao *et al.* 2010). Some studies clearly show that *M. avidus* has a
564 continuous paroral membrane; only in the first phases of stomatogenesis (during the
565 transformation of microstomes into to macrostomes), the paroral membrane is divided,
566 with a small segment at the posterior end (Gómez-Saladín & Small, 1993a).

567 The morphology of oral polykinetids M1, M2, and M3 in isolates Pe5 and Pe7
568 and *Philasterides dicentrarchi* strain I1 is very similar to that observed in *M. avidus*; but
569 differs from the oral polykinetids of congeners. the M1 of isolates Pe5 and Pe7 and

570 strain I1 of *P. dicentrarchi* is elongated like the M1 of *M. avidus* (Thompson &
571 Moewus, 1964), while the M1 of *P. armata* and *P. armatalis* is usually triangular
572 (Grolière 1980; Song *et al.* 2000); the M3 in *P. dicentrarchi* strain I1 and in the isolates
573 Pe5 and Pe7 is irregularly triangular and similar to *M. avidus* (Thompson & Moewus,
574 1964), but different from the rectangular M3 of *P. armata* (Grolière, 1980).

575 During early and late phases of equal fission, most ciliates share certain features,
576 such as common position of macronucleus and micronucleus, synchronization of
577 macronuclear amitosis and fission furrow, and a specific and well defined dividing size
578 (Long & Zufall, 2010). The position of the micronucleus relative to the macronucleus is
579 not specified in the original descriptions of *P. dicentrarchi* and *M. avidus*, which only
580 states that the micronucleus is closely associated with the macronucleus but completely
581 separate from it in *P. dicentrarchi* (Dragesco *et al.* 1995; Paramá *et al.* 2006); however,
582 some later descriptions proposed the anterior position of the micronucleus relative to the
583 macronucleus as a specific characteristic of *M. avidus* (Hu *et al.* 2009). In this study, we
584 clearly demonstrate that the position of the micronucleus relative to the macronucleus in
585 Pe5, Pe7 isolates and in strain I1 of *P. dicentrarchi* is very variable.

586 The formation of tomites, which is a general characteristic of scuticociliates,
587 occurs in response to starvation without cyst production, or in response to drugs
588 (Fenchel, 1987; Gómez-Saladín & Small, 1993b, Morais *et al.* 2009). *Miamiensis*
589 *avidus* is a known tomite-producing scuticociliate (Thompson & Moewus, 1964;
590 Gómez-Saladín & Small, 1993a; b). The life cycles of scuticociliates provide further
591 taxonomically significant features. While *M. avidus* undergoes microstome to
592 macrostome transformation following a considerable change in cell size and the buccal
593 structures (Small, 1967; Gómez-Saladín & Small, 1993a), such a transformation was
594 not observed in *P. dicentrarchi* (Dragesco *et al.* 1995). In the present study, we

595 performed tomitogenesis and prey-induced transformation experiments with *M. avidus*
596 strain Ma/2, *P. dicentrarchi* strain I1 isolated from *P. adspersus*, and isolate Pe7 in a
597 nutrient-depleted medium. We observed induction of the macrostome forms only in *M.*
598 *avidus* strain Ma/2, and in co-cultures of this strain Ma/2 with the *P. dicentrarchi* strain
599 I1; however, this phenomenon does not occur when I1 trophozoites were incubated with
600 trophozoites of isolates (Pe7) of fine flounder, and neither macrostome forms nor any
601 sign of predation/cannibalism could be detected.

602 The scuticociliate isolates Pe5 and Pe7 from the fine flounder *P. adspersus* and
603 *P. dicentrarchi* strain I1 are obviously virulent in their hosts; however, the infective
604 capacity of the *M. avidus* strain Ma/2, which has been maintained in culture for a long
605 time (more than 40 years) in the ATCC collection (Soldo & Merlin, 1972), in unknown
606 In the present study, we demonstrated the high virulence of the strain Ma/2, causing a
607 mortality of 100% in turbot after experimental infection.

608 Identification of scuticociliates only on the basis of morphological features may
609 lead to misidentification (Whang *et al.* 2013). To solve this problem, molecular
610 techniques, mainly on the analysis of the small subunit rRNA gene (SSUrRNA) are
611 used. Besides barcoding for identification, they also enable clarification of the
612 phylogenetic relationships and the taxonomy of scuticociliates (Gao *et al.* 2012). The
613 phylogenetic analysis reveal a cluster of *P. dicentrarchi* strains I1 and isolates Pe7 and
614 Pe5 as sister group of strains YK2 and YS2, which from olive flounder, that had been
615 identified as *M. avidus* (syn. *P. dicentrarchi*) (Song & Wilbert, 2000; Jung *et al.* 2007)
616 and whose SSUrRNA gene sequence data have been described in previous studies by
617 Jung *et al.* (2005) and Song *et al.* (2009a; b). *Miamiensis avidus* strain Ma/2, which is
618 considered to represent the “real” *M. avidus* and the isolate FXP2009050602, a strain
619 that is very morphologically similar to *M. avidus* described by Song & Wilbert (2000),

620 but differs in some morphological characteristics, and shows great differences at the
621 molecular level with the strains from Korea (Jung *et al.* 2011; Gao *et al.* 2012), together
622 and both are related to *Anopryoides haemophila*, a species that has already been
623 included with *M. avidus* in the family Paraaronematidae on the basis of SSUrRNA
624 topologies (Gao *et al.* 2012). These results therefore indicate that the Peruvian isolates
625 from *P. adspersus* are similar to *P. dicentrarchi* and closely related to strains YK2 and
626 YS2; however, they are phylogenetically most distant from strain Ma/2 and isolate
627 FXP2009050602 of *M. avidus*. To corroborate this, we compared the α/β tubulin gene
628 sequences in *P. dicentrarchi* and *M. avidus* strain Ma/2 held in the ATCC and isolate
629 FXP2009050602 of *M. avidus* provide valuable information about the taxonomic
630 position of the species analyzed (Stoeck *et al.* 2000; Schmidt *et al.* 2006; Barth *et al.*
631 2006; Budiño *et al.* 2011a). α - and β -tubulin genes are suitable phylogenetic markers
632 discriminating strains and investigate the intraspecific genetic variability in *P.*
633 *dicentrarchi* (Budiño *et al.* 2011a). The nucleotide sequences identity of 99% and 100%,
634 respectively in the α - and β -tubulin genes, indicate a conspecificity. The differences
635 between the *P. dicentrarchi* strains and *M. avidus* strain Ma/2 were also confirmed at
636 serological level. Although serological tests are widely used for identification in other
637 protozoa (de Waal, 2012), they are not usually used to diagnose ciliate infections in fish.
638 Nonetheless, they have proved very useful for characterizing and distinguishing antigens
639 from *P. dicentrarchi* and *M. avidus*, expressed during infection in turbot and in olive
640 flounder, and thus to differentiate strains (Piazzon *et al.* 2008; Song *et al.* 2009b;
641 Budiño *et al.* 2012). These findings confirm the above-mentioned genetic findings on
642 comparing the nucleotide sequences of the gene encoding this protein.

643 Final conclusion. The morphological analysis, tomitogenesis and prey-induced
644 transformation, comparisons of SSUrRNA and α/β tubulin gene sequences, and

645 serological analysis all clearly indicate that isolates Pe5 and Pe7 and *P. dicentrarchi*
646 strain I1 are not conspecific with *M. avidus* strain Ma/2 (ATCC). We also found that *P.*
647 *dicentrarchi* displayed low identity in SSUrRNA sequences with *P. armatalis*. The low
648 identity (based on the nucleotide sequences of this gene) between *P. dicentrarchi* and *P.*
649 *armatalis* was also described by Gao *et al.* (2012).

650 Until the nucleotide sequences of the 18S gene of the type species *P. armatalis*
651 becomes available, we cannot definitely confirm that this species belongs to the genus
652 *Philasterides*, or whether it should be transferred to another genus, or even propose its
653 inclusion in a new genus.

654 The analysis of SSUrRNA gene sequences indicates that *P. dicentrarchi*
655 obtained from turbot and fine flounder (I1, Pe5 and Pe7) and isolates YK2 and YS2
656 from olive flounder of *Miamiensis avidus* are the same ciliate species, suggesting
657 that the latter have been misidentified. Morphological analysis of all of these
658 isolates is therefore urgently required for their correct identification.

659 In conclusion, the aetiological agent of scuticociliatosis produced in the fine
660 flounder *Paralichthys adspersus* is the same as that described in the olive flounder
661 *Paralichthys. olivaceus* and the turbot *S. maximus*. Due to the lack of information
662 regarding the nucleotide sequence of the SSUrRNA gene in the type species of
663 *Philasterides*, we suggest that the name *P. dicentrarchi* should be maintained for the
664 species that causes scuticociliatosis in turbot and fine flounder.

665

666 ACKNOWLEDGEMENTS

667 We are grateful for the support provided by Jaime Pauro (Headship of Pacific
668 Aquaculture Deep Frozen S A-Perú-) and by Dr Violeta Flores and Marco Medina of
669 the IMERPA (Peru) for technical assistance with scuticociliate isolation. This study was

670 financially supported by grant AGL2014-57125-R from the Ministerio de Economía y
671 Competitividad (Spain), by grant GPC2014/069 from the Xunta de Galicia (Spain) and
672 by PARAFISHCONTROL project. This project received funding from the *European*
673 *Union's Horizon 2020 research and innovation programme* under grant agreement No.
674 634429. This publication reflects the views only of the authors, and the European
675 Commission cannot be held responsible for any use, which may be made of the
676 information contained therein.

677

678 REFERENCES

- 679 **Azad, I.S., Al-Marzouk, A., James, C.M., Almatar, S. and Al-Gharabally, H.**
680 (2007). Scuticociliatosis-associated mortalities and histopathology of natural
681 infection in cultured silver pomfret (*Pampus argenteus* Euphrasen) in Kuwait.
682 *Aquaculture* **262**, 202–210.
- 683 **Bart, D., Drenek, S., Fokin, S. and Berendonk, T.U.** (2006). Intraspecific genetic
684 variation in *Paramecium* revealed by mitochondrial cytochrome c oxidase I
685 sequences. *Journal of Eukaryotic Microbiology* **53**, 20-25.
- 686 **Bonar, C.J., Garner, M.M., Weber, E.S., Keller, C.J., Murray, M., Adams, L.M.a**
687 **and Frasca S. Jr.** (2013). Pathologic findings in weedy (*Phyllopteryx*
688 *taeniolatus*) and leafy (*Phycodurus eques*) seadragons. *Veterinary Pathology* **50**,
689 368-376.
- 690 **Bordier, C.** (1981). Phase separation of integral membrane proteins in Triton X-114.
691 *The Journal of Biological Chemistry*, **256**,1604-1607.
- 692 **Budiño, B., Lamas, J., Pata, M.P., Arranz, J.A., Sanmartín, M.L. and Leiro, J.**
693 (2011a). Intraspecific variability in several isolates of *Philasterides dicentrarchi*

- 694 (syn. *Miamiensis avidus*), a scuticociliate parasite of farmed turbot. *Veterinary*
695 *Parasitology* **175**, 260-272.
- 696 **Budiño, B., Lamas, J., González, A., Pata, M.P., Devesa, S., Arranz, J.A. and Leiro,**
697 **J.** (2011b). Coexistence of several *Philasterides dicentrarchi* strains on a turbot
698 fish farm. *Aquaculture* **322-323**, 23-32.
- 699 **Budiño, B., Leiro, J., Cabaleiro, S. and Lamas, J.** (2012). Characterization of
700 *Philasterides dicentrarchi* isolates that are pathogenic to turbot: serology and
701 cross-protective immunity. *Aquaculture*, **364-365**, 130-136.
- 702 **de Waal, T.** (2012). Advances in diagnosis of protozoan diseases. *Veterinary*
703 *Parasitology* **189**, 65-74.
- 704 **Declercq, A.M., Chiers, K., Van den Broeck, W., Rekecki, A., Teerlinck, S.,**
705 **Adriaens, D., Haesebrouck, F. and Decostere, A.** (2014). White necrotic tail
706 tips in estuary seahorses, *Hippocampus kuda*, Bleeker. *Journal of Fish Diseases*
707 **37**, 501-504.
- 708 **di Cicco, E., Paradis, E., Stephen, C., Turba, M.E. and Rossi, G.** (2013).
709 Scuticociliatid ciliate outbreak in Australian potbellied sea horse, *Hippocampus*
710 *abdominalis* (Lesson, 1827): clinical signs, histopathological findings, and
711 treatment with metronidazole. *Journal of Zoo and Wildlife Medicine* **44**, 435-440.
- 712 **Dickerson, H.W., Clark, T.G. and Findly, R.C.** (1989). *Ichthyophthirius multifiliis*
713 has membrane-associated immobilization antigens. *The Journal of Protozoology*
714 **36**, 159-164.
- 715 **Dragesco, A., Dragesco, J., Coste, F., Gasc, C., Romestand, B., Raymond, J. and**
716 **Bouix, G.** (1995). *Philasterides dicentrarchi*, n. Sp. (Ciliophora,
717 Scuticociliatida), a histiophagous opportunistic parasite of *Dicentrarchus labrax*

- 718 (Linnaeus, 1758), a reared marine fish. *European Journal of Protistology* **31**,
719 327-340.
- 720 **Fan, X., Hu, X., Al-Farraj, S.A., Clamp, J.C. and Song W.** (2011). Morphological
721 description of three marine ciliates (Ciliophora, Scuticociliatia), with
722 establishment of a new genus and two species. *European Journal of Protistology*
723 **47**, 186-196.
- 724 **Felsenstein, J.** (1985). Confidence limits on phylogenies: and approach using the
725 bootstrap. *Evolution* **39**, 783-791.
- 726 **Fenchel, T.** (1987). Adaptative significance of polymorphic life cycles in protozoa:
727 resposes to starvation and reffeding in two species of marine ciliates. *Journal of*
728 *Experimental Marine Biology and Ecology* **136**, 159-177.
- 729 **Fernández-Galiano, D.** (1994). The ammoniacal silver carbonate method as a general
730 procedure in the study of protozoa from sewage (and other) waters. *Water*
731 *Research* **28**, 495-496.
- 732 **Gao, F., Fan, X., Yi, Z., Strüder-Kypke, M. and Song, W.** (2010). Phylogenetic
733 consideration of two scuticociliate genera, *Philasterides* and *Boveria* (Protozoa,
734 Ciliophora) based on 18 S rRNA gene sequences. *Parasitology International* **59**,
735 549-555.
- 736 **Gao, F., Katz, L.A. and Song W.** (2012). Insights into the phylogenetic and taxonomy
737 of philasterid ciliates (Protozoa, Ciliophora, Scuticociliatia) based on analyses of
738 multiple molecular marker. *Molecular Phylogenetics and Evolution* **64**, 308-317.
- 739 **Gao, F., Katz, L.A. and Song, W.** (2013). Multigene-based analyses on evolutionary
740 phylogeny of two controversial ciliate orders: Pleuronematida and
741 Loxocephalida (Protista, Ciliophora, Oligohymenophorea). *Molecular*
742 *Phylogenetics and Evolution* **68**, 55-63.

- 743 **Gómez-Saladín, E. and Small, E.B.** (1993a). Oral morphogenesis of the microstome to
744 macrostome transformation in *Miamiensis avidus* strain Ma/2. *Journal of*
745 *Eukaryotic Microbiology* **40**, 363-370.
- 746 **Gómez-Saladín, E. and Small, E.B.** (1993b). Starvation induces tomitogenesis in
747 *Miamiensis avidus* strain Ma/2. *Journal of Eukaryotic Microbiology* **40**, 727-730.
- 748 **Grolière, C.A.** (1980). Morphologie et stomatogenèse chez deux ciliés Scuticociliatida des
749 genres *Philasterides* Kahl, 1926 et *Cyclidium* O. F. Müller; 1786. *Acta*
750 *Protozoologica* **19**, 195-206.
- 751 **Harikrishnan, R., Balasundaram, C. and Heo, M.S.** (2010). Scuticociliatosis and its
752 recent prophylactic measures in aquaculture with special reference to South
753 Korea Taxonomy, diversity and diagnosis of scuticociliatosis: Part I Control
754 strategies of scuticociliatosis: Part II. *Fish and Shellfish Immunology* **29**, 15-31.
- 755 **Harikrishnan, R., Jin, C.N., Kim, J.S., Balasundaram, C. and Heo, M.S.** (2012).
756 *Philasterides dicentrarchi*, a histophagous ciliate causing scuticociliatosis in
757 olive flounder, *Philasterides dicentrarchi* –Histopathology investigations.
758 *Experimental Parasitology* **130**, 239-245.
- 759 **Hu, X., Song, W. and Warren, A.** (2009). Scuticociliatids. In. Free-living Ciliates in
760 Bohai and Yellow Sea, China. (Song W., Warren A. & Hu X. ,eds.) Science
761 Press. Beijing.
- 762 **Iglesias, R., Paramá, A., Álvarez, M.F., Leiro, J., Fernández, J. and Sanmartín,**
763 **M.L.** (2001). *Philasterides dicentrarchi* (Ciliophora, Scuticociliatida) as the
764 causative agent of scuticociliatosis in farmed turbot, *Scophthalmus maximus* in
765 Galicia (NW Spain). *Diseases of Aquatic Organisms* **46**, 47-55.

- 766 **Iglesias, R., Paramá, A., Álvarez, M.F., Leiro, J., Aja, C. and Sanmartín, M.L.**
767 (2003a). *In vitro* growth requirements for the fish pathogen *Philasterides*
768 *dicentrarchi* (Ciliophora, Scuticociliatida). *Veterinary Parasitology* **111**, 19-30.
- 769 **Iglesias, R., Paramá, A., Álvarez, M.F., Leiro, J., Ubeira, F.M. and Sanmartín,**
770 **M.L.** (2003b). *Philasterides dicentrarchi* (Ciliophora: Scuticociliatida) express
771 surface immobilization antigens that probably induce protective immune
772 responses in turbot. *Parasitology* **126**, 125-134.
- 773 **Ito, H., Fukuda, Y., Murata, K. and Kimura, A.** (1983). Transformation of intact
774 yeast cells treated with alkali cations. *Journal of Bacteriology* **153**, 163–168.
- 775 **Jung, S.J., Kitamura, S.I., Song, J.Y., Joung, I.Y. and Oh, M.J.** (2005). Complete
776 small subunit rRNA gene sequence of the scuticociliate *Miamiensis*
777 *avidus* pathogenic to olive flounder *Paralichthys olivaceus*. *Diseases of Aquatic*
778 *Organisms* **64**, 159–162.
- 779 **Jung, S.J., Kitamura, S.I., Song, J.Y. and Oh, M.J.** (2007). *Miamiensis avidus*
780 (Ciliophora: Scuticociliatida) causes systemic infection of olive flounder
781 *Paralichthys olivaceus* and is a senior synonym of *Philasterides dicentrarchi*.
782 *Diseases of Aquatic Organisms* **73**, 227-234.
- 783 **Jung, S.J., Im, E.Y., Struder-Kypke, M.C., Kitamura, S. and Woo, P.T.** (2011).
784 Small subunit ribosomal RNA and mitochondrial cytochrome c oxidase subunit
785 1 gene sequences of 21 strains of the parasitic scuticociliate *Miamiensis avidus*
786 (Ciliophora, Scuticociliatia). *Parasitology Research* **108**, 1153-1161.
- 787 **Kim, S.M., Cho, J.B., Kim, S.K., Nam, Y.K. and Kim, K.H.** (2004a). Occurrence of
788 scuticociliatosis in olive flounder *Paralichthys olivaceus* by *Philasterides*
789 *dicentrarchi* (Ciliophora: scuticociliatia). *Diseases of Aquatic Organisms* **62**,
790 2333-2338..

- 791 **Kaneshiro, E.S., Dunham, P.B. and Holz, G.G.** (1969). Osmorregulation in a marine
792 ciliate, *Miamiensis avidus*. I. Regulation of inorganic ions and water. *The*
793 *Biological Bulletin* **136**, 65-75.
- 794 **Kimura, M.** (1980). A simple method for estimating evolutionary rates of base
795 substitutions through comparative studies of nucleotide sequences. *Journal of*
796 *Molecular Evolution* **16**, 111-120.
- 797 **Kumar, S., Stecher, G., and Tamura, K.** (2016). MEGA7: Molecular Evolutionary
798 Genetics Analysis version 7.0 for bigger datasets. *Molecular Biology and*
799 *Evolution* **33**: 1870-1873.
- 800 **Leiro, J., Siso, M.I., Paramá, A., Ubeira, F.M. and Sanmartín, M.L.** (2000). RFLP
801 analysis of PCR-amplified small subunit ribosomal DNA of three fish
802 microsporidian species. *Parasitology* **124**, 145-151.
- 803 **Long, H. and Zufall, R.A.** (2010). Diverse modes of reproduction in the marine free-
804 living ciliate *Glauconema trihymene*. *BioMed Central Microbiology* **10**, 108.
- 805 **López-López, O., Fuciños, P., Pastrana, L., Rúa, M.L., Cerdán, M.E. and**
806 **González-Siso, M.I.** (2010). Heterologous expression of an esterase from
807 *Thermus thermophilus* HB27 in *Saccharomyces cerevisiae*. *Journal of*
808 *Biotechnology* **145**, 226-232.
- 809 **Lynn, D.H. and Strüder-Kypke, M.** (2005). Scuticociliate endosymbionts of echinoids
810 (phylum Echinodermata): phylogenetic relationships among species in the
811 genera *Entodiscus*, *Plagiopyliella*, *Thyrophylax*, and *Entorhipidium* (phylum
812 Ciliophora). *The Journal of Parasitology* **91**, 1190-1199.
- 813 **McWilliam, H., Li, W., Uludag, M., Squizzato, S., Park, Y.M., Buso, N., Cowley,**
814 **A.P., and López, R.** (2013). Analysis tool web services from the EMBL-EBI.
815 *Nucleic Acids Research* **41**(Web Server issue), W597-W600.

- 816 **Mallo, N., Lamas, J. and Leiro, J.M.** (2013). Evidence of an alternative oxidase
817 pathway for mitochondrial respiration in the scuticociliate *Philasterides*
818 *dicentrarchi*. *Protist* **164**, 824-836.
- 819 **Mallo, N., Lamas, J., Piazzon, C. and Leiro, J.M.** (2015). Presence of a plant-like
820 proton-translocating pyrophosphatase in a scuticociliate parasite and its role as a
821 possible drug target. *Parasitology* **142**, 449-462.
- 822 **Mallo, N., Lamas, J., Defelipe, A.P., Decastro, M.E., Sueiro, R.A. and Leiro, J.M.**
823 (2016). Presence of an isoform of H⁺-pyrophosphatase located in the alveolar
824 sacs of a scuticociliate parasite of turbot: physiological consequences.
825 *Parasitology* **143**, 576-587.
- 826 **Miao, M., Warren, A., Song, W., Wang, S., Shang, H. and Chen, Z.** (2008). Analysis
827 of internal transcribed spacer 2 (ITS2) region of scuticociliates and related taxa
828 (Ciliophora, Oligohymenophorea) to infer their evolution and phylogeny. *Protist*
829 **159**, 519-533.
- 830 **Miao, M., Wang, Y., Song, W., Clamp, J. C., and Al-Rasheid, K. A. S.** (2010).
831 Description of *Eurystomatella sinica* n. gen., n. sp., with establishment of a new
832 family Eurystomatellidae n. fam. (Protista, Ciliophora, Scuticociliatia) and
833 analyses of its phylogeny inferred from sequences of the small-subunit rRNA
834 gene. *International Journal of Systematic and Evolutionary Microbiology* **60**,
835 460-468
- 836 **Moewus, L.** (1963). Studies on a marine parasitic ciliate as a potential virus vector. In:
837 Symp. on Marine Microbiology. pp. 366-379. C.H. Oppenheimer (Ed.), Charles
838 C. Thomas, Springfield, Ill.

- 839 **Morais, P., Lamas, J., Sanmartín, M.L., Orallo, F. and Leiro, J.** (2009).
840 Resveratrol induces mitochondrial alterations, autophagy and a cryptobiosis-
841 like state in scuticociliates. *Protist* **160**, 552-564.
- 842 **Moustafa, E.M.M., Naota, M., Morita, T., Tange, N. and Shimada, A.** (2010).
843 Pathological study on the scuticociliatosis affecting farmed Japanese flounder
844 (*Paralichthys olivaceus*) in Japan. *The Journal of Veterinary Medical Science* **72**,
845 1359-1362.
- 846 **Munday, B.L., O'Donoghue, P.J., Watts, M., Rough, K. and Hawkesford, T.** (1997).
847 Fatal encephalitis due to the scuticociliate *Uronema nigricans* in sea-caged,
848 southern bluefin tuna *Thunnus maccoyii*. *Diseases of Aquatic Organisms* **30**, 17-
849 25.
- 850 **Ofelio, C., Blanco, A., Roura, A., Pintado, J., Pascual, S. and Planas, M.** (2014).
851 Isolation and molecular identification of the scuticociliate *Porpostoma notata*
852 Moebius, 1888 from moribund reared *Hippocampus hippocampus* (L.) seahorses,
853 by amplification of the SSU rRNA gene sequences. *Journal of Fish Diseases* **37**,
854 1061-1065.
- 855 **Pan, X., Zhu, M., Ma, H., Al-Rasheid, K.A. and Hu, X.** (2013). Morphology and
856 small-subunit rRNA gene sequences of two novel marine ciliates, *Metanophrys*
857 *orientalis* spec. nov. and *Uronemella sinensis* spec. nov. (Protista, Ciliophora,
858 Scuticociliatia), with an improved diagnosis of the genus *Uronemella*.
859 *International Journal of Systematic and Evolutionary Microbiology* **63**, 3515-23.
- 860 **Paramá, A., Iglesias, R., Álvarez, M.F., Leiro, J., Aja, C. and Sanmartín, M.L.**
861 (2003). *Philasterides dicentrarchi* (Ciliophora, Scuticociliatida): experimental
862 infection and possible routes of entry in farmed turbot (*Scophthalmus maximus*).
863 *Aquaculture* **217**, 73-80.

- 864 **Paramá, A., Arranz, J.A., Álvarez, M.F., Sanmartín, M.L. and Leiro, J.** (2006).
865 Ultrastructure and phylogeny of *Philasterides dicentrarchi* (Ciliophora:
866 Scuticociliatia) from farmed turbot in NW Spain. *Parasitology* **132**, 555-564.
- 867 **Paramá, A., Castro, R., Lamas, J., Sanmartín, M.L., Santamarina, M.T., and Leiro,**
868 **J.** (2007). Scuticociliate proteinases may modulate turbot immune response by
869 inducing apoptosis in pronephric leucocytes. *International Journal for*
870 *Parasitology* **37**, 87-95.
- 871 **Piazzon, C., Lamas, J., Castro, R., Budiño, B., Cabaleiro, S., Sanmartín, M.L., and**
872 **Leiro, J.** (2008). Antigenic and cross-protection studies on two turbot
873 scuticociliate isolates. *Fish and Shellfish Immunology* **25**, 417-424.
- 874 **Piazzon, C., Lamas, J. and Leiro, J.M.** (2011). Role of scuticociliate proteinases in
875 infection success in turbot, *Psetta maxima* (L.). *Parasite Immunology* **33**, 535-
876 544.
- 877 **Ramos, M.F., Costa, A.R., Barandela, T., Saraiva, A. and Rodrigues, P.N.** (2007).
878 Scuticociliate infection and pathology in cultured turbot *Scophthalmus maximus*
879 from the north of Portugal. *Diseases of Aquatic Organisms* **74**, 249-253.
- 880 **Rossteucher, S., Wenker, C., Jermann, T., Wahli, T., Oldenberg, E. and Schmidt-**
881 **Posthaus, H.** (2008). Severe scuticociliate (*Philasterides dicentrarchi*) infection
882 in a population of sea dragons (*Phycodurus eques* and *Phyllopteryx taeniolatus*).
883 *Veterinary Parasitology* **45**, 546-550.
- 884 **Schmidt, S.L., Benhart, D., Schlegel, M. and Fried, J.** (2006). Fluorescence *in situ*
885 with specific oligonucleotide rRNA probes distinguishes the sibling species
886 *Stylonychia lemnaea* and *Stylonychia mytilus* (Ciliophora, Spirotrichea). *Protist*
887 **157**, 21-30.

- 888 **Shin, P.S., Han, J.E., Gómez, D.K., Kim, J.H., Choresca, Jr. C.H., Jun, J.W., and**
889 **Park, S.C.** (2011). Identification of scuticociliate *Philasterides dicentrarchi*
890 from indo-pacific seahorses *Hippocampus kuda*. *African Journal of*
891 *Microbiology Research* **5**, 738-741.
- 892 **Sievers, F., Wilm, A., Dineen, D., Gibson, T.J., Karplus, K., Li, W., López,**
893 **R., McWilliam, H., Remmert, M., Söding, J., Thompson, J.D. and Higgins,**
894 **D.G.** (2011). Fast, scalable generation of high-quality protein multiple sequence
895 alignments using Clustal Omega. *Molecular Systems Biology* **7**, 539.
- 896 **Saitou, N. and Nei M.** (1987). The neighbor-joining method: A new method for
897 reconstructing phylogenetic trees. *Molecular Biology and Evolution* **4**, 406-425.
- 898 **Small, E.B.** (1967). The scuticociliatida, a new Order onf the Class Ciliatea (Phylum
899 Protozoa, Subphylum Ciliophora). *Transactions of the American Microscopical*
900 *Society* **86**, 345-370.
- 901 **Small, H.J., Neil, D.M., Taylor, A.C., Bateman, K. and Coombs, G.H.** (2005). A
902 parasitic scuticociliate infection in the Norway lobster (*Nephrops norvegicus*).
903 *Journal of Invertebrate Pathology* **90**, 108-117.
- 904 **Smith, P.J., McVeagh, S.M., Hulston, D., Anderson, S.A. and Gublin, Y.** (2009).
905 DNA identification of ciliates associated with disease outbreaks in a New
906 Zealand marine fish hatchery. *Diseases of Aquatic Organisms* **86**, 163-167.
- 907 **Soldo, A.T. and Merlin, E.J.** (1972). The cultivation of symbiont-free marine ciliates
908 in axenic medium. *The Journal of Protozoology* **19**, 519-524.
- 909 **Song, W.B. and Wilbert, N.** (2000). Redefinition and redescription of some marine
910 scuticociliates from China, with report of a new species, *Metanophrys siensis*
911 nov. Spec. (Ciliophora, Scuticociliatida). *Zoologischer Anzeiger* **239**, 45-74.

- 912 **Song, J.Y., Kitamura, S., Oh, M.J., Kang, H.S., Lee, J.H., Tanaka, S.J., and Jung,**
913 **S.J.** (2009a). Pathogenicity of *Miamiensis avidus* (syn. *Philasterides*
914 *dicentrarchi*), *Pseudocohnilembus persalinus*, *Pseudocohnilembus hargisi*
915 and *Uronema marinum* (Ciliophora, Scuticociliatida). *Diseases of Aquatic*
916 *Organisms* **83**, 133-143.
- 917 **Song, J.Y., Sasaki, K., Okada, T., Sakashita, M., Kawahami, H., Matsuoka, S., Kan,**
918 **H.S., Nakayama, K., Jung, S.J., Oh, M.J. and Kitamura, S.I.** (2009b).
919 Antigenic differences of the scuticociliate *Miamiensis avidus* from Japan.
920 *Journal of Fish Diseases* **32**, 1027-1034.
- 921 **Stidworthy, M.F., Garner, M.M., Bradway, D.S., Westfall, B.D., Joseph, B.,**
922 **Repetto, S., Guglielmi, E., Schmidt-Posthaus, H. and Thornton, S.M.** (2014).
923 Nondomestic, exotic, wildlife and zoo animals systemic scuticociliatosis
924 (*Philasterides dicentrarchi*) in sharks. *Veterinary Pathology* **51**, 628-663.
- 925 **Stoeck, T., Welter, H., Seitz-Bender, D., Kusch, J. and Schmidt, H.J.** (2000).
926 ARDRA and RAPD-fingerprint reject the sibling species concept for the ciliate
927 *Paramecium caudatum* (Ciliophora, Protoctista). *Zoologica Scripta* **29**, 75-82.
- 928 **Thompson, J.C., and Moewus, L.** (1964). *Miamiensis avidus* n. g., n. sp., a marine
929 facultative parasite in the ciliate order Hymenostomatida. *The Journal of*
930 *Protozoology* **11**, 378-381.
- 931 **Umehara, A., Kosuga, Y. and Hirose, H.** (2003). Scuticociliata infection in the weedy
932 sea dragon *Phyllopteryx taeniolatus*. *Parasitology International* **52**, 165-168.
- 933 **Whang, I., Kang, H.S. and Lee, J.** (2013). Identification of scuticociliates
934 (*Pseudocohnilembus persalinus*, *P. longisetus*, *Uronema marinum* and
935 *Miamiensis avidus*) based on the cox1 sequence. *Parasitology International* **62**,
936 7-13.

937 **Figures and Table legends**

938 **Figure 1.** *Paralichthys adspersus*: clinical signs of infection. (A) Visible changes are
939 observed in the pigmentation of infected fish, and (B) the presence of
940 haemorrhagic lesions on the gills. (C) Ciliates obtained from ascites liquid.
941 Histopathological findings of the infection by scuticociliates: (D) Histological
942 section of gills showing the presence of ciliates (arrows), and (E)
943 microphotograph showing a massive infection of ciliates in the myocardium
944 (arrows) causing intense cardiac muscle histophagy. Staining H&E, scale bar =
945 50 μ M.

946 **Figure 2.** Morphological characteristics of isolates Pe5 and Pe7 from farmed flounder
947 *Paralichthys adspersus* in comparison with those of *Miamiensis avidus* strain
948 Ma/2 (ATCC[®] 50180TM). Silver carbonate-impregnated trophozoites: isolate Pe5
949 (A,B); isolate Pe7 (F, G); and *Miamiensis avidus* strain Ma/2 (ATCC[®] 50180TM)
950 (J, M, N). (A, F) Light micrographs showing the oral ciliature and the posterior
951 cell portions (B,G) of isolates Pe5 and Pe7, respectively. (C, D, H) Schematic
952 drawings of the buccal apparatus in *Philasterides dicentrarchi* from sea bass (C),
953 Pe5 (D), and Pe5 (H), showing three oral polykinetids, (M1, M2 and M3) and
954 two paraoral membrane (PM1 and PM2) (E, I) Drawings of posterior ends of
955 isolates Pe5 and Pe7 showing 12 kineties (1-12), the pore of the subterminal
956 contractile vacuole (VP), and a prominent caudal cilium (C, circle). (J) Light
957 microphotograph of silver carbonate-impregnated specimens of *M. avidus* strain
958 Ma/2 showing the buccal apparatus. (K, L) Drawings of oral ciliature in *M.*
959 *avidus* from original description (K) and strain Ma/2 (L) showing the oral
960 polykinetids M1, M2 and M3, and the paraoral membrane (PM). (M)
961 Microphotograph of a trophozoite of *M. avidus* strain Ma/2 showing the spine-

962 shaped apical cell portion (arrow). (N, O) Tomites of *M. avidus* strain Ma/2
 963 stained with silver-carbonate (N), and *in vivo* under phase contrast optics (O).
 964 Scale bars = 10 μ m.

965 **Figure 3.** Structure of nuclear apparatus. Confocal microscope photomicrographs (A, B,
 966 D) of trophozoites stained with DAPI, and light micrographs of cells stained
 967 with silver carbonate (C), showing the position of the macronucleus (M) and
 968 micronucleus (m): (A) strain I1 of *Philasterides dicentrarchi*, (B) isolate Pe5, (C)
 969 isolate Pe7, and (D) strain Ma/2 of *Miamiensis avidus*. Figure C also shows the
 970 caudal cilium (c) and the posterior contractile vacuole (cv). Scale bars = 10 μ m.

971 **Figure 4.** Induction of tomitogenesis in *M. avidus* and *P. dicentrarchi* under conditions
 972 of starvation. Cultures of *M. avidus* (A, B) and *P. dicentrarchi* (C, D), in media
 973 with nutrients (A, C) and without nutrients in non-nutrient artificial seawater (B,
 974 D). M: macrostomes; m: microstomes; t: tomites. Scale bar = 10 μ m.

975 **Figure 5.** (A) Prey-induced transformation of *M. avidus* ATCC[®] 50180[™] (strain Ma/2)
 976 co-cultivated with the I1 strain from *Philasterides dicentrarchi* in non-nutrient
 977 artificial seawater (NSS). (A-D) Macrostome formation at day 2 of co-cultures
 978 showing ciliates ingested in its interior (circles and arrows). (A) Silver staining,
 979 (B) phase contrast, (C) acridine orange staining, (D) DAPI staining. (E)
 980 Polymerase chain reaction from genomic DNA of *M. avidus* (M), *P.*
 981 *dicentrarchi* strain I1 (I1), and *M. avidus* and *P. dicentrarchi* (M+I1) co-
 982 cultivated for five days. (F) Primers designed from the nucleotide sequences of *P.*
 983 *dicentrarchi* corresponding to (a) the α -tubulin, (b) β -tubulin and (c) the small
 984 rRNA subunit (SSUrRNA) gene used for PCR. Mw: molecular size markers.

985 **Figure 6.** Virulence of the Ma / 2 strain of *M. avidus* ATCC[®] 50180[™] in
 986 experimentally infected turbot. (A) Abdominal distension due to accumulation

987 of ascitic fluid in the body cavity. The arrow indicates anal inflammation. (B)
988 Kinetics of cumulative mortality induced after intraperitoneal injection with *M.*
989 *avidus* five after infection.

990 **Figure 7.** Neighbour-joining (NJ) unrooted trees inferred from: SSUrRNA (A), as well
991 as, the α - (B), and β -tubulin (C) nucleotide sequences showing the phylogenetic
992 relationships between isolates Pe5 and Pe7 from the fine flounder, strain I1 of
993 *Philasterides dicentrarchi* isolated from turbot, and strain Ma/2 of *Miamiensis*
994 *avidus* ATCC[®] 50180[™]. The phylogeny was also inferred by analysis of
995 SSUrRNA gene sequences between the isolates from the fine flounder, strains of
996 *Philasterides* isolated from turbot, strains of *Miamiensis* isolated from olive
997 flounder (strains YK2 and YS2), isolate FXP2009050602 of *M. avidus*, and
998 several species of philasterids (see Table 1) including strain GF200806601 of
999 *Philasterides armatalis* (A). Nodes represent bootstrap values of 1000 resampled
1000 values in the NJ analysis with the Kimura two-parameter correction model, and
1001 the scale bar indicates the genetic distance.

1002 **Figure 8.** Analysis of the antigenic relationships related to the alpha subunit of tubulin,
1003 using a gene fragment (A) between isolates from the fine flounder *P. adspersus*,
1004 *Philasterides dicentrarchi* strain I1 and *Miamiensis avidus* strain Ma/2 (ATCC[®]
1005 50180[™]), by various immunoassays using antibodies generated against a
1006 fragment of recombinant α -tubulin. Immunopattern recognition by
1007 immunofluorescence: (B) vs. *P. dicentrarchi* strain I1 (confocal microscope
1008 image using a combined DAPI staining and staining with FITC), (C) vs. the Pe5
1009 isolate (D) and the Pe7 isolate from the fine flounder *P. adspersus* and, (E) vs. *M.*
1010 *avidus* strain Ma/2. (F) ELISA of the degree of cross-reactivity between α -
1011 tubulin from *P. dicentrarchi* strain I1, isolate Pe7 from the fine flounder *P.*

1012 *adpersus* and *M. avidus* strain Ma/2. The results are expressed as mean values
 1013 of the absorbance at 492 nm \pm standard error (n=5), and asterisks indicate the
 1014 statistical significance ($P < 0.01$). (G) Western blot analysis of ciliary proteins of
 1015 *M. avidus* strain Ma/2 (lane 1), *P. dicentrarchi* strain I1 (lane 2) and the Pe7
 1016 isolate from *P. adpersus* showing two bands of recognition corresponding to
 1017 two polypeptide fragments of α -tubulin (arrows). Mw: molecular weight
 1018 markers expressed in kD.

1019 **Table 1.** List of philasterid species included in the phylogenetic analysis, showing the
 1020 GenBank Accession numbers for their SSUrRNA gene sequences, the
 1021 isolates/strains, host specificity, and sequence length in base pairs (bp).

1022 **Table 2.** Biometric data for silver-impregnated ciliates isolates (Pe5 and Pe7) from
 1023 *Paralichthys adpersus*, *Philasterides dicentrarchi* strain I1 isolated from turbot,
 1024 *P. dicentrarchi* (Dragesco et al., 1995) from seabass, strains T5 and T16 of
 1025 *Miamiensis avidus* (Thompson and Moewus 1964), and strain Ma/2 of *M. avidus*
 1026 (ATCC[®] 50180[™]). *Biometric values obtained from specimens of *M. avidus*
 1027 supplied by ATCC and cultured in our laboratory. †Data obtained from
 1028 microstomes. The values shown are expressed (in μm) as mean \pm standard error,
 1029 with the minimum-maximum ranges in parentheses. M1-M3: oral polykinetids,
 1030 PM: paroral membrane; PM1, PM2: paroral membranes 1 and 2. CVP:
 1031 contractile vacuole pore; Kn: kinety. The measurements were made in 50
 1032 specimens. (-) No data available.

1033 **Table 3.** Nucleotide identity percentage analyzed by the BLAST alignment program
 1034 between regions of DNA gene of the small subunit of (A) rRNA (SSUrRNA)
 1035 and (B) α - and β -subunits of tubulin of isolates Pe5 and Pe7 from the fine
 1036 flounder *Paralichthys adpersus*, strain I1 of *Philasterides dicentrarchi* isolated

1037 from turbot and strain Ma/2 of *Miamiensis avidus* held in ATCC[®] 50180[™].
1038 Additionally, the BLAST analysis of the SSUrRNA sequences included the
1039 strains YK2 and YS2 of *Miamiensis avidus* isolated from *Paralichthys olivaceus*,
1040 and the GF2008082801 strain of *Philasterides armatalis*.

For Peer Review

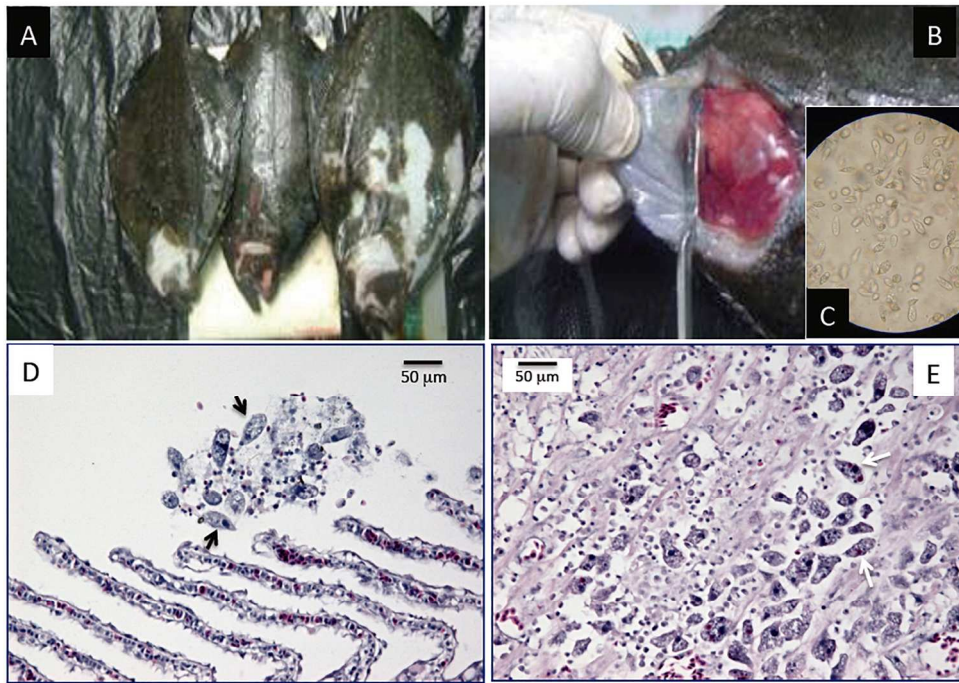


Figure 1

209x150mm (300 x 300 DPI)

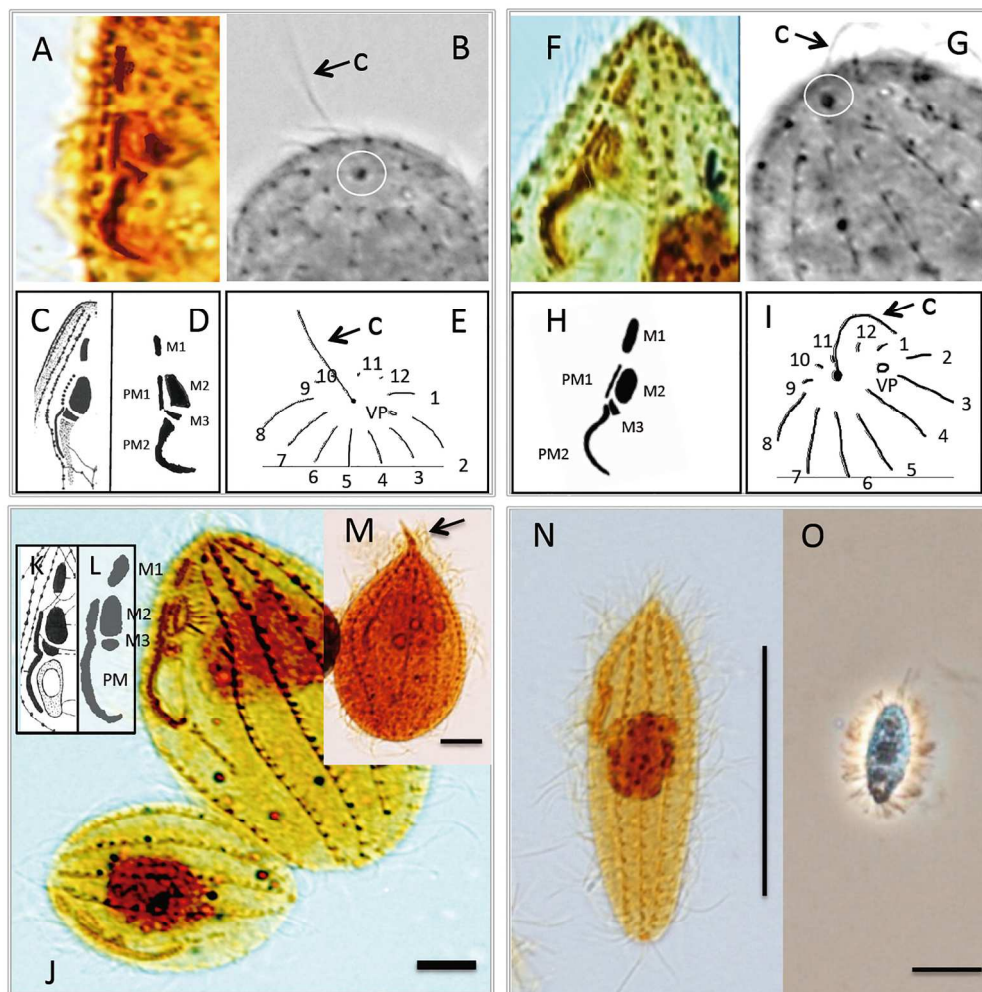


Figure 2

209x214mm (300 x 300 DPI)

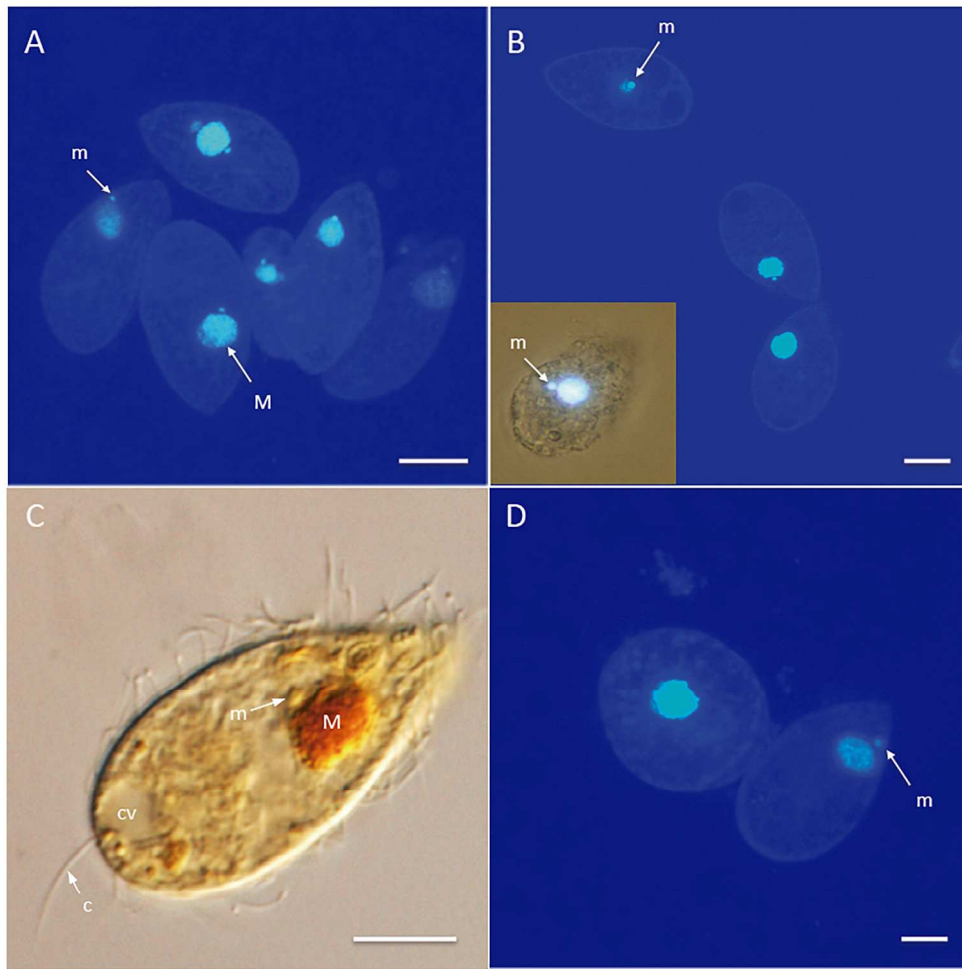


Figure 3

209x210mm (300 x 300 DPI)

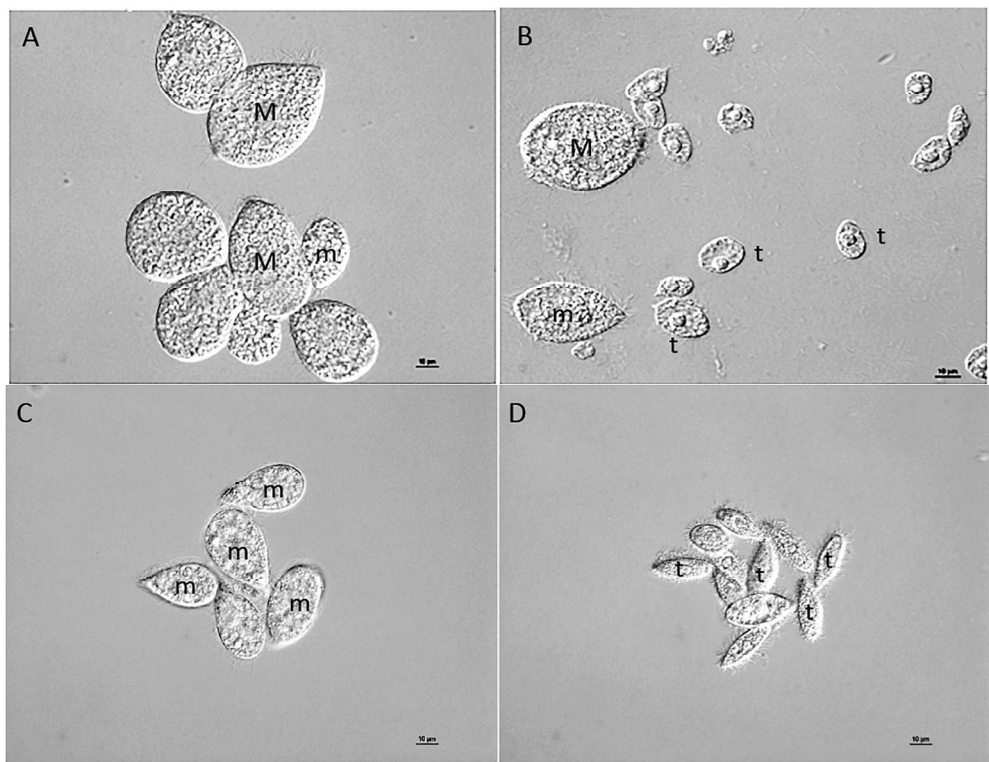


Figure 4

209x162mm (300 x 300 DPI)

Review

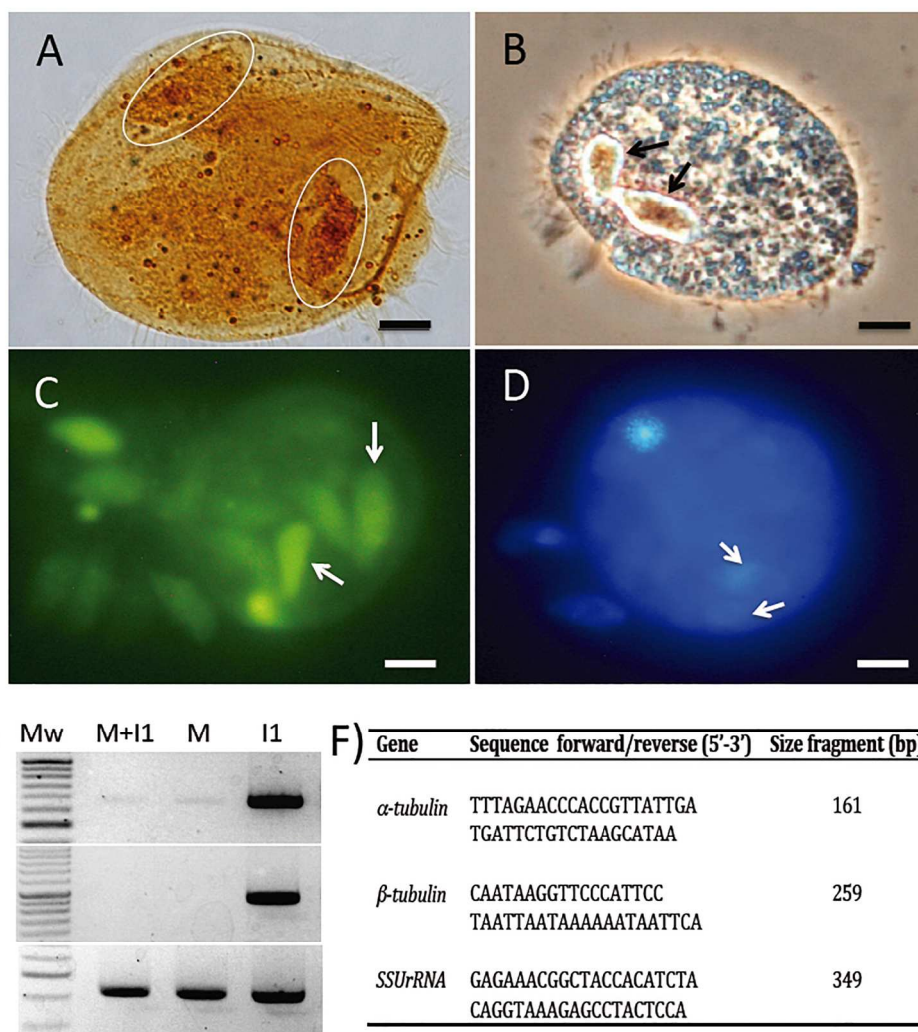


Figure 5

209x220mm (300 x 300 DPI)

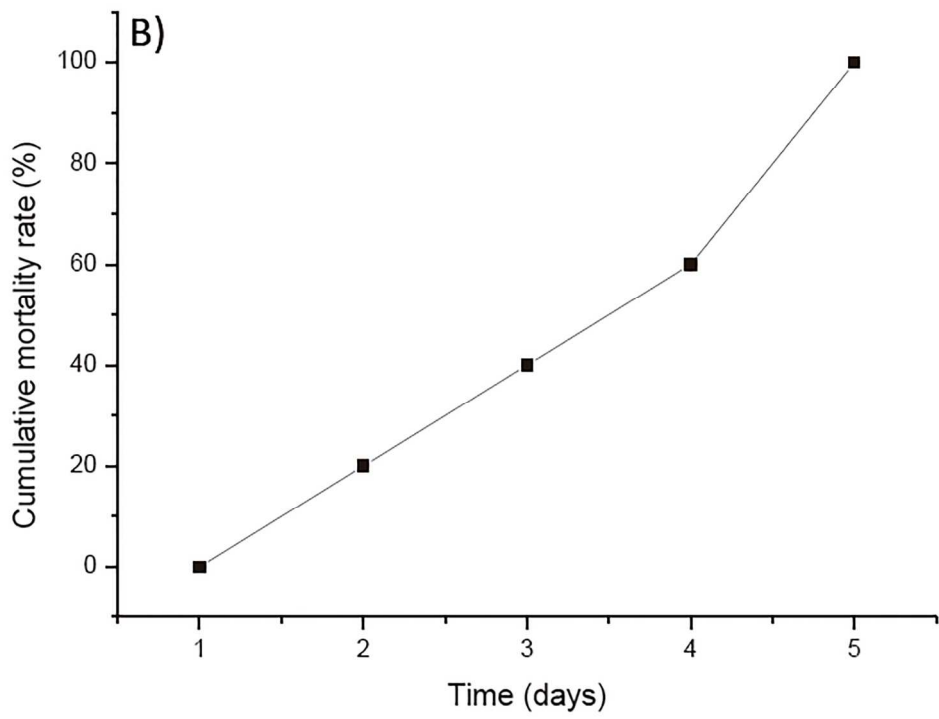
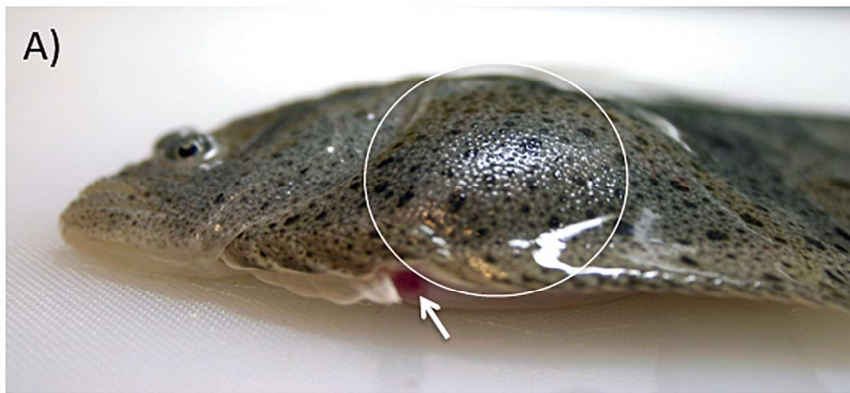


Figure 6

209x242mm (300 x 300 DPI)

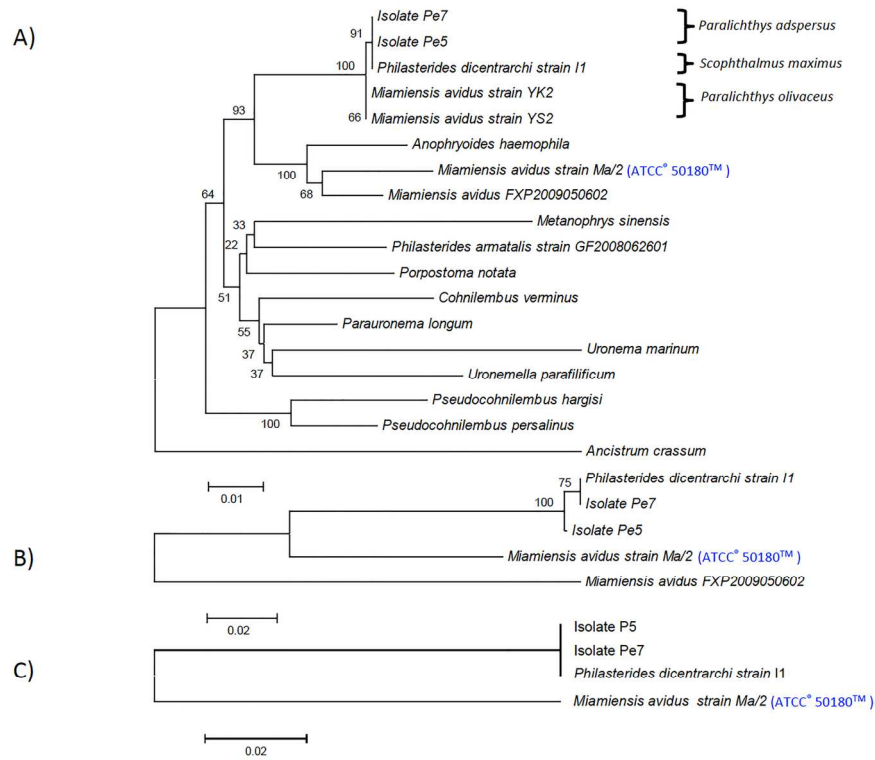


Figure 7

167x133mm (300 x 300 DPI)

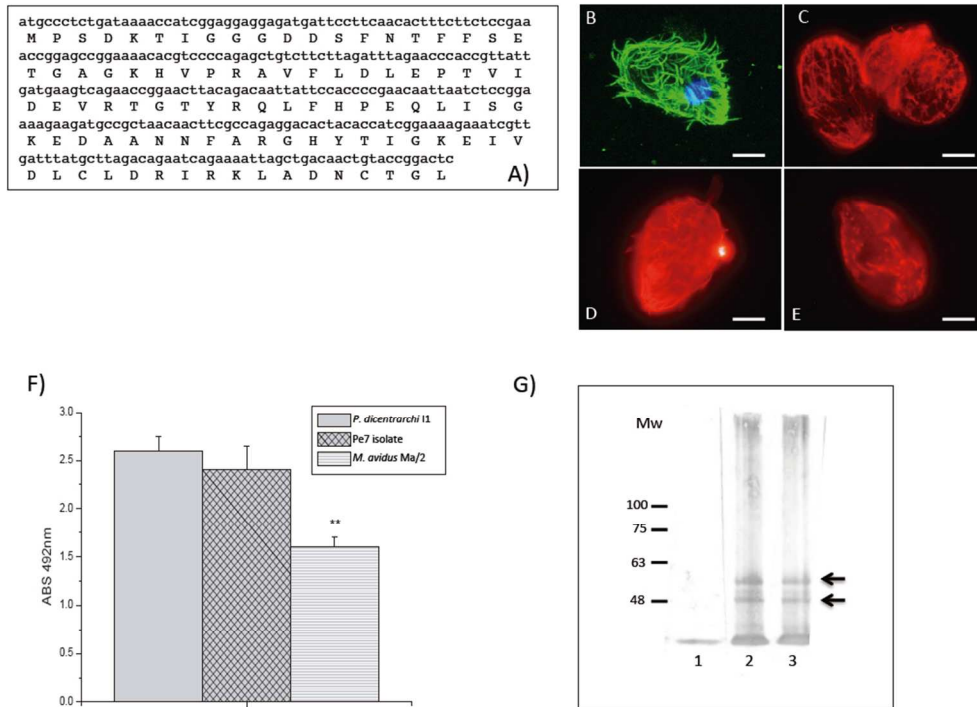


Figure 8

87x64mm (300 x 300 DPI)

| Species | Accession number | Isolate/strain | Host | Size (bp) |
|---|------------------|----------------|---|-----------|
| <i>Ancistrum crassum</i> | HM236340 | FXP2009051101 | - | 1753 |
| <i>Anophryoides haemophila</i> | U51554.1 | - | Lobster, <i>Homarus americanus</i> | 1763 |
| <i>Metanophrys sinensis</i> | HM236336 | FXP2009052901 | - | 1554 |
| <i>Miamiensis avidus</i> ATCC [®] 50180 [™] | KX357144 | Ma/2 | Seahorses | 1759 |
| <i>Miamiensis avidus</i> | EU831208 | YK2 | Olive flounder, <i>Paralichthys olivaceus</i> | 1759 |
| <i>Miamiensis avidus</i> | EU831200 | YS2 | Olive flounder, <i>Paralichthys olivaceus</i> | 1759 |
| <i>Miamiensis avidus</i> | JN885091.1 | FXP2009050602 | - | 1760 |
| <i>Parauronema longum</i> | HM236338 | FXP200903150 | - | 1759 |
| <i>Philasterides dicentrarchi</i> | JX914665 | I1 | Turbot, <i>Scophthalmus maximus</i> | 1759 |
| <i>Philasterides armatalis</i> | FJ848877 | GF2008062601 | - | 1758 |
| <i>Porpostoma notata</i> | HM236335 | FXP2009050601 | Seahorses, <i>Hippocampus hippocampus</i> | 1755 |
| <i>Pseudocohnilembus hargisi</i> | AY833087 | SCL-B | Olive flounder, <i>Paralichthys olivaceus</i> | 1752 |
| <i>Pseudocohnilembus persalinus</i> | AY835669 | SCL-A | Olive flounder, <i>Paralichthys olivaceus</i> | 1754 |
| <i>Uronema marinum</i> | GQ465466 | PHB090219 | Marine fishes | 1758 |
| <i>Uronemella parafilificum</i> | HM236337 | FXP2009053001 | - | 1756 |

| Characteristics | Pe5 isolate | Pe7 isolate | <i>Philasterides dicentrarchi</i> strain I1 | <i>Philasterides dicentrarchi</i> | <i>Miamiensis avidus</i> | <i>Miamiensis avidus</i> strain Ma/2* | |
|---------------------------------|-------------------------------|-------------------------------|---|-----------------------------------|--|---------------------------------------|---------------------------------------|
| Body dimensions | | | | | | | |
| Length [†] | 39.5 ± 4.5 (25-48) | 34.6 ± 5.9 (25-51) | 33.6 ± 4.2 (25-43) | 35.1 ± 4.8 (23-43) | 31.9 | 39.9 | 40.2 ± 4.2 (34-46) |
| Width [†] | 21.5 ± 3.7 (16-28) | 19.6 ± 3.8 (12-29) | 19.5 ± 3.0 (15-28) | 18.5 ± 2.5 (12-25) | 16.1 | 20.1 | 23.4 ± 2.6 (18-28) |
| Size of nuclei | | | | | | | |
| Macronucleus | 5.4 ± 0.8 (4-6) | 5.9 ± 1.2 (3-8) | 7.0 ± 1.0 (5-9) | 6.4 ± 1.1 (4-8) | 4.1 | 5.1 | 13.2 ± 2.6 (6-17) |
| Micronucleus | 1.0 ± 0.2 (0.6-1.2) | 1.2 ± 0.3 (0.7-1.6) | 1.6 ± 0.2 (1.3-1.9) | 1.5 ± 0.2 (1.2-1.8) | Exist | Exist | 1.7 ± 0.3 (1.4-2.0) |
| Somatic cilia | | | | | | | |
| Total no. of kineties | 10-12 | 10-13 | 13-14 | 14 (13-15) | 10-12 | 10-13 | 9-11 |
| Oral ciliature | | | | | | | |
| Dist. from apex to M1 | 3.0 ± 1.1 (1.6-4.3) | 3.5 ± 0.6 (3.03-4.6) | 3.9 ± 0.5 (2.5-5.0) | 3.7 ± 0.7 (3-5) | 3-4 | 3-4 | 3.3 ± 1.9 (1.4-10.9) |
| Length of buccal field | 14.4 ± 2.4 (9.2-17.6) | 12.8 ± 2.2 (8.6-18.3) | 18.8 ± 1.3 (15.3-22.1) | - | 13.6 | 17.1 | 17.7 ± 3.1 (8.9-23.9) |
| Length of PM1 | 3.2 ± 0.5 (2.4-3.9) | 3.1 ± 1.3 (2.2-4.3) | 3.7 ± 0.5 (2.5-4.8) | 4.1 ± 0.5 (3.5-5) | 7.5 Sometimes a narrow gap | 9.9 Sometimes a narrow gap | 12.7 ± 3.1 (6.9-18.5) (continuous) |
| Length of PM2 | 8.1 ± 7.9 (4.4-10.2) | 5.9 ± 1.2 (2.2-7.8) | 6.25 ± 1.6 (4.6-7.9) | 6.0 ± 1.0 (4.5-8) | - | - | - |
| Length M1 | 1.2 ± 0.4 (0.9-1.5) | 1.6 ± 0.3 (0.9-1.8) | 2.0 ± 1.2 (2.0-2.9) | 2.3 ± 0.3 (2-3) | 2.6 | 3 | 2.75 ± 0.7 (1.4-3.8) |
| Length M2 | 1.6 ± 0.3 (1.2-2.1) | 1.8 ± 0.4 (1.2-2.4) | 3.1 ± 1.8 (2.7-3.5) | 2.9 ± 0.4 (2-4) | 2.8 | 3.6 | 3.5-0.9 (1.3-4.9) |
| Length M3 | 0.5 ± 0.2 (0.2-0.9) | 0.4 ± 0.1 (0.3-0.7) | 0.8 ± 0.5 (0.7-1.0) | 1.8±0.3 (1.2-2.1) | 1.1 | 1 | 1.5±0.4 (0.6-2.3) |
| Buccal field/Body length | 0.4 ± 0.1 (0.3-0.5) | 0.4 ± 0.1 (0.3-0.5) | 0.4 ± 0.1 (0.4-0.5) | - | 0.4 | 0.4 | 0.4 ± 0.1 (0.35-0.55) |
| Position of CVP | Posterior end of kinety 2 | Posterior end of kinety 2 | Posterior end of kinety 2 | Between kinety 1 & 2 | Posterior end of kinety 2 (occasionally 2 CVP's at the base of kinety 2 and 3) | | Posterior end of kinety 2 |
| Characteristics of Kn | Terminate at M1 | Terminate at M1 | Terminate at M1 | Terminate at M1 | Terminate at M1 | | Terminate at M1 |
| Sample location | Huarmey, Perú | Huarmey, Perú | Galicia, Spain | Montpellier, France | Miami, U.S.A. | | Miami, USA |
| Host | <i>Paralichthys adspersus</i> | <i>Paralichthys adspersus</i> | <i>Scophthalmus maximus</i> | <i>Dicentrarchus labrax</i> | Sea horses?-local bay waters of Miami, Florida- | | Sea horses |
| Life cycle | Microstome/tomite | Microstome/tomite | Microstome/tomite | - | - | | Macrostome/microstome/tomite |
| Data source | Present study | Present study | Present study | Dragesco et al. (1995) | Thompson & Moewus (1964) | | Present study |

| | <i>M. avidus</i> strain Ma/2 | <i>P. dicentrarchi</i> isolate Pe5 | <i>P. dicentrarchi</i> isolate Pe7 | <i>P. dicentrarchi</i> strain I1 | <i>M. avidus</i> strain YK2 | <i>P. armatalis</i> strain GF2008082801 |
|---|---------------------------------|---------------------------------------|---------------------------------------|-------------------------------------|--------------------------------|--|
| 5 | 96% | | | | | |
| 7 | 96% | 100% | | | | |
| | 96% | 100% | 100% | | | 95% |
| | 96% | 99% | 99% | 99% | | 95% |
| | 96% | 99% | 99% | 99% | 99% | 95% |
| 2 | 97% | 96% | 96% | 96% | 96% | 95% |

| | <i>M. avidus</i> strain Ma/2 | <i>P. dicentrarchi</i> isolate Pe5 | <i>P. dicentrarchi</i> isolate Pe7 | <i>P. dicentrarchi</i> strain I1 |
|-------|-----------------------------------|---------------------------------------|---------------------------------------|-------------------------------------|
| Pe5 | $\alpha = 89\%$ $\beta = 85\%$ | | | |
| Pe7 | $\alpha = 89\%$ $\beta = 85\%$ | $\alpha = 99\%$ $\beta = 100\%$ | | |
| I1 | $\alpha = 89\%$ $\beta = 85\%$ | $\alpha = 99\%$ $\beta = 99\%$ | $\alpha = 100\%$ $\beta = 99\%$ | |
| 50602 | $\alpha = 83\%$ | $\alpha = 82\%$ | $\alpha = 81\%$ | $\alpha = 81\%$ |

Supplementary Material: nucleotide sequences used

| Specie | strain | gene | Accession number | Nucleotide sequence | Length (bp) |
|---------------------------------------|--------|---|------------------|--|-------------|
| <i>Philasterides dicentrarchi</i> | 11 | 18S ribosomal RNA gene, complete sequence | JX914665.1 | AATCTGGTTGATCCTGCCAGTAGTCATATGCTTGTCTCAAAGATTAAGCCATGCATGTCTAAGTATAAATAGTATACAGTGAAACT GCGAATGGCTCATTAAAACAGTTATAGTTTATTTGATAATGGAAAGCTACATGGATAACCGTGGTAATCTAGAGCTAATACATGC TGTCAAACCCGACCTTTGGAAAGGTTGATTTATTAGATATTAAGCCAATATTCCTTCGGGTCTATTGGTGAATCATAGTAACT GATCGAATCTCTTACAGAGATAAATCATTCAAGTTTCTGCCATCAGCTTTTCGATGGTAGTGTATTGGACTACCATGGCAGTCAC GGGTAACGGAGAATTAGGGTTCGGTTCCGGAGAGGGAGCCTGAGAAACGGCTACCACATCTAAGGAAGGCAGCAGGCGCGTA AATTACCCAATCCTGATTACGGAGGTAGTGACAAGAAATAACAACCTGGGGGCCTCACGGCCTACGGGATTGAATGAGAAC AATTTAAACGACTTAACGAGGAACAATTGGAGGGCAAGTCTGGTCCAGCAGCCGCGTAATCCAGCTCCAATAGCGTATATT AAAGTTGTTGCAGTTAAAAGCTCGTAGTTGAACCTTCTGCATGTGCCAGTCTGGCTTCGGTCAAGCTGTGGTGTATGCATCCG CTTGCAAAGCTAGACCGTCTTATTGATCGACTAGTGGAGTAGGCTCTTACCTTGAAAAATTAGAGTGTTCAGGCAGGCAA TGGCTCGAATACATTAGCATGGAATAATGGAATAGGACTTTTGTCCATTTGGTTGGTATTGGACATAAGTAATGATTAAGGGA CAGTTGGGGCATTAGTATTTAATGTCAGAGGTGAAATCTTGGATTTATTAAGACTAATATGCGAAAGCATTGGCAAGGA TGTTTTCATTAATCAAGAACGAAAGTTAGGGGATCAAAGACGATCAGATACCGTCTAGTCTTAACATAAACTATACCGACTCGG AATCGGACCGGCTTATAAACTGGTTCGGCGCGTATGAGAAATCAAAGTCTTTGGTTCTGGGGGAGTATGGTCCGAAGGCT GAAACTTAAGGAATTGACGGAAGGGCACCACAGGCGTGGAGCTGCGGCTAATTTGACTCAACACGGGAAACTTACCAG GTCCAAACATGGGTGGGATTGACAGATTGAGAGCTCTTCTTGATTCTATGGGTGGTGGTGCATGGCCGTTCTAGTTGGTGA GTGATTTGCTGGTTAATCCGTTAACGAACGAGACCTTAACCTGCTAAATAGTACGTTGATGCACAATGGCGTTACTTCTTAGA GGGACTATGCGCTTTGAAACGCATGGAAGTTTGAAGCAATAACAGGCTGTGATGCCCTTAGATGTCCTGGGCGCACGCGCG CTACAATGACTCGCTCAGAAAGTACTTCTGGTCCGGAAGGATTGGGTAATCTTTAAATACGAGTCGTGTAGGGATCGATCT TTGTAATTATGGATCTGAACGAGGAATGCCTAGTAAGTCAAGTCAATCAGCTTGTACTGATTACGTCCTCCCTTTGTACACA CCGCCGTCGCTCCTACCGATTTGAGTGTATCCGGTGAACCTTCTGGACTGAGCAGCCTTGCCTGAACGGGAAGTTAAGTAAAC CTAATCACTTAGAGGAAGGAGAAGTCGTAACAAGGTTTCCGTAGGTGAACCTGCGGAAGGATC | 1759 |
| <i>Miamiensis avidus</i> ATCC® 50180™ | Ma/2 | 18S ribosomal RNA gene, complete sequence | KX357144 | AATCTGGTTGATCCTGCCAGTAGTCATATGCTTGTCTCAAAGATTAAGCCATGCATGTCTAAGTATAAATAGTATACAGTGAAACT GCGAATGGCTCATTAAAACAGTTATAGTTTATTTGATAATGGAAAGCTACATGGATAACCGTGGTAATCTAGAGCTAATACATGC TGTTAAGCCTGACTTTTTGGGAGGGCTGTATTTATTAGATATTAAGCCAATATTCCTTGTGTCTATTGGTGAATCATAGTAACT GATCGAATCTCTTTTTGAGATAAATCATTCAAGTTTCTGCCATCAGCTTTTCGATGGTAGTGTATTGGACTACCATGGCAGTTAC GGGTAACGGAGAATTAGGGTTCGGTTCCGGAGAGGGAGCCTGAGAAACGGCTACCACATCTAAGGAAGGCAGCAGGCGCGTA AATTACCCAATCCTGATTACGGAGGTAGTGACAAGAAATAACAACCTGGGGGACTTTGTCCCTTACGGGATTGCAATGAGAACA TTTAAACGACTTATCGAGGAACAATTGGAGGGCAAGTCTGGTCCAGCAGCCGCGTAATCCAGCTCCAATAGCGTATATTA AGTTGTTGCAGTTAAAAGCTCGTAGTTGAATTTCTGTACATGACTGGTTCTGGCCTCGGTCAAGCCTGTTCTGTGCATCCGCT TGCAAACTGGGACCGGTATTCAATTCGACCCAGGGAGTAGGCCCTTACCTTGAAAAATAGAGTGTTCAGGCAGGCAATT GCTCGAATACATTAGCATGGAATAATAGAATAGGACTTTTGTCCATTTGGTTGTTATTGGACATGAGTAATGATTAAGGGGACA GTTGGGGCATTAGTATTTAATTGTCAGAGGTGAAATCTTGGATTTATTAAGACTAATCTATGCGAAAGCATTGGCAAGGATG TTTTCATTAATCAAGAACGAAAGTTAGGGGATCAAAGACGATCAGATACCGTCTAGTCTTAACATAAACTATACCGACTCGGAA TCGGCAGGCTAATAAATCTTGTCCGGCCTGATGAAAATCAAAGTCTTTGGTTCTGGGGGAGTATGGTCCGCAAGGCTGAA ACTTAAGGAATTGACGGAAGGGCACCACAGGCGTGGAGCTGCGGCTAATTTGACTCAACACGGGAAACTTACCAGGTC CAAACATGGGTGGGATTGACAGATTGAGAGCTCTTCTTGATTCTATGGGTGGTGGTGCATGGCCGTTCTAGTTGGTGGAGT ATTTGCTGGTTAATCCGTTAACGAACGAGACCTTAACCTGCTAAATAGTAGCCTTATGAACAATGGGGTTACTTCTTAGAGG ACTATCGTTTTGAATCGCATGGAAGTTTGAAGCAATAACAGGCTCTGTGATGCCCTTAGATGTCCTGGGCGCAGCGCGCTAC AATGATTCGCTCAGAAAGTATTTCTGGCCGGAAGGGTTCAGGGTAATCTTTCAATACGAATCGTGTAGGGATCGATCTTTG CAATTATAGATCTGAACGAGGAATGCCTAGTAAGTCAAGTCAATCAGCTTGTACTGATTACGTCCTCCCTTTGTACACACCC CCCGTCGCTCCTACCGATTTGAGTGTATCCGGTGAACCTTCTGGACCGAGAGCGCTTGCCTCATGGGAAGTTAAGTAAACCTA ATCACTTAGAGGAAGGAGAAGTCGTAACAAGGTTTCCGTAG GTGAACCTGCGGAAGGATC | 1759 |
| Isolates Pe5 | - | 18S ribosomal | - | AATCTGGTTGATCCTGCCAGTAGTCATATGCTTGTCTCAAAGATTAAGCCATGCATGTCTAAGTATAAATAGTATACAGTGAAACT GCGAATGGCTCATTAAAACAGTTATAGTTTATTTGATAATGGAAAGCTACATGGATAACCGTGGTAATCTAGAGCTAATACATGC | 1759 |

| | | | | | |
|---------------------------------------|------|--------------------------------|----------|--|-----|
| | | partial sequence | | GGAATCCATGGTACCGGGTTCCAAATCCATAAGGATGGCTC | |
| <i>Miamiensis avidus</i> ATCC® 50180™ | Ma/2 | Beta tubulin, partial sequence | KX357147 | CCATAATTCTGTCGGGGTATTCTTCTCTGACTTTGGAGATAAGGAGGGTACCCATTCCGGATCCAGTTCCTCCTCCAAGAGAGTG GGTGATTAGAAACCTTATAAGCAATCACATCCTTCGGCTTCTTTCTGACGACATCCAAAACGGAGTCGATCAATTCAGCTCCTT CGGTGTAATGACCTTTGGCCAGTTGTTACCAGCTCCAGTTTGCCGAAAACGCTATTATAAAAATAAAATTAATATTTTCTCAGTTT TTAATATATTTCAATGTGATTTACAAGTTATCGGGTCTGAAGAGTTGACCGAAAAGTCCAGCTCTACGGAATCCATGGTCCGG GTTCCGAGATCCATTAAGATGGCTCTGGGAACGTATCTTCTCCG | 388 |
| Pe5 isolate | - | Beta tubulin, partial sequence | - | CCATAATTCTGTCGGGGTATTCTTCTCTGACTTTGGAGATCAATAAGGTTCCCATTCGGATCCAGTTCCTCCTCCTAAAGAGTG GGTGATTAGAAACCTTATAAGCAATCACATCCTTCAGCTTCTTTCTGACAACATCTAAAACAGAGTCGATTAATTCAGCTCCTTC GGTGTAGTGTCTTTGGCCAGTTGTTACCAGCTCCGGTTTATCCGAAAACGCTATTTAATTATTTAATTTAATTACATCTTTCT TCATTATATAAAACAATTGAATTTATTTTATTAATTATTACAAGTTATCAGGTCTGAAGAGTTGTCGAAAAGTCCAGCTCTAAC GGAATCCATGGTACCGGGTTCCAAATCCATAAGGATGGCTC | 388 |
| Pe7 isolate | - | Beta tubulin, partial sequence | - | CCATAATTCTGTCGGGGTATTCTTCTCTGACTTTGGAGATCAATAAGGTTCCCATTCGGATCCAGTTCCTCCTCCTAAAGAGTG GGTGATTAGAAACCTTATAAGCAATCACATCCTTCAGCTTCTTTCTGACAACATCTAAAACAGAGTCGATTAATTCAGCTCCTTC GGTGTAGTGTCTTTGGCCAGTTGTTACCAGCTCCGGTTTATCCGAAAACGCTATTTAATTATTTAATTTAATTACATCTTTCT TCATTATATAAAACAATTGAATTTATTTTATTAATTATTACAAGTTATCAGGTCTGAAGAGTTGTCGAAAAGTCCAGCTCTAAC GGAATCCATGGTACCGGGTTCCAAATCCATAAGGATGGCTC | 388 |